



**HAL**  
open science

## Dynamic single-cell phenotyping of immune cells using the microfluidic platform DropMap

Yacine Bounab, Klaus Eyer, Sophie Dixneuf, Magda Rybczynska, Cécile Chauvel, Maxime Mistretta, Trang Tran, Nathan Aymerich, Guilhem Chenon, Jean-François Litjos, et al.

### ► To cite this version:

Yacine Bounab, Klaus Eyer, Sophie Dixneuf, Magda Rybczynska, Cécile Chauvel, et al.. Dynamic single-cell phenotyping of immune cells using the microfluidic platform DropMap. *Nature Protocols*, 2020, 15 (9), pp.2920-2955. 10.1038/s41596-020-0354-0 . hal-03054278

**HAL Id: hal-03054278**

**<https://hal.science/hal-03054278v1>**

Submitted on 31 Dec 2020

**HAL** is a multi-disciplinary open access archive for the deposit and dissemination of scientific research documents, whether they are published or not. The documents may come from teaching and research institutions in France or abroad, or from public or private research centers.

L'archive ouverte pluridisciplinaire **HAL**, est destinée au dépôt et à la diffusion de documents scientifiques de niveau recherche, publiés ou non, émanant des établissements d'enseignement et de recherche français ou étrangers, des laboratoires publics ou privés.

1 **FILE NOT INTENDED FOR PRODUCTION**

2 **Dynamic Single-Cell Phenotyping of Immune Cells using the Microfluidic**  
3 **Platform DropMap**

4  
5 Yacine Bounab<sup>1,2§</sup>, Klaus Eyer<sup>3,4§</sup>, Sophie Dixneuf<sup>1</sup>, Magda Rybczynska<sup>3</sup>, Cécile Chauvel<sup>1</sup>, Maxime Mistretta<sup>1</sup>  
6 ,Trang Tran<sup>1</sup>, Nathan Aymerich<sup>3</sup>, Guilhem Chenon<sup>3</sup>, Jean-François Llitjos<sup>5</sup>, Fabienne Venet<sup>6,7</sup>, Guillaume  
7 Monneret<sup>6,7</sup>, Iain Gillespie<sup>8</sup>, Pierre Cortez<sup>9</sup>, Virginie Moucadel<sup>6,10</sup>, Alexandre Pachot<sup>10</sup>, Alain Troesch<sup>1</sup>, Philippe  
8 Leissner<sup>1</sup>, Julien Textoris<sup>6,10,11</sup>, Jérôme Bibette<sup>3</sup>, Cyril Guyard<sup>1</sup>, Jean Baudry<sup>3\*</sup>, Andrew D. Griffiths<sup>2\*</sup> and  
9 Christophe Védrine<sup>1\*</sup>.

10 <sup>1</sup>BIOASTER Technology Research Institute, Lyon, France.

11 <sup>2</sup>Laboratoire de Biochimie (LBC), École Supérieure de Physique et de Chimie Industrielles de la Ville de Paris  
12 (ESPCI Paris), Université Paris Sciences et Lettres (PSL), CNRS UMR8231, Paris, France.

13 <sup>3</sup>Laboratoire de Colloïdes et Matériaux Divisés (LCMD), École Supérieure de Physique et de Chimie Industrielles  
14 de la Ville de Paris (ESPCI Paris), Université Paris Sciences et Lettres (PSL), CNRS UMR8231, Paris, France.

15 <sup>4</sup>Laboratory for Functional Immune Repertoire Analysis, Institute of Pharmaceutical Sciences, D-CHAB, ETH  
16 Zürich, Zürich.

17 <sup>5</sup>Medical intensive care unit of Cochin hospital, Paris, France.

18 <sup>6</sup>EA7426 “Pathophysiology of Injury-induced immunosuppression”, Université Claude Bernard Lyon-1 - HCL-  
19 bioMérieux, Lyon, France.

20 <sup>7</sup>Immunology Laboratory, Hospices Civils de Lyon, Lyon, France.

21 <sup>8</sup>GlaxoSmithKline, Brentford, Middlesex, UK.

22 <sup>9</sup>R&D, Sanofi Aventis, Chilly-Mazarin, France.

23 <sup>10</sup>Medical Diagnostic Discovery Department (MD3), bioMérieux S.A., France.

24 <sup>11</sup>Anesthesiology and Critical Care Medicine, HCL, Lyon, France.

25 <sup>§</sup>These authors contributed equally

26 \*e-mail: jean.baudry@espci.fr, andrew.griffiths@espci.fr and christophe.vedrine@bioaster.org

27  
28 Correspondence to:

29 Dr Christophe Védrine, BIOASTER Technology Research Institute, Bâtiment François Jacob, 28, rue du Docteur  
30 Roux, 75015 Paris, France. Email: christophe.vedrine@bioaster.org.

31 Pr Andrew D Griffiths, Laboratoire de Biochimie (LBC), ESPCI Paris, PSL Université, CNRS UMR8231, Paris,  
32 France. Email: andrew.griffiths@espci.fr

33 Dr Jean Baudry, Laboratoire de Colloïdes et Matériaux Divisés (LCMD), ESPCI Paris, PSL Université, CNRS  
34 UMR8231, Paris, France. Email: jean.baudry@espci.fr

35 **EDITORIAL SUMMARY** This protocol describes a microfluidic platform for dynamic high-throughput  
36 analysis the phenotype of single cells. Cell-surface markers and secreted proteins are quantified and  
37 characterized by fluorescence detection using tailored immunoassays, simultaneously with  
38 measurement of other cellular characteristics, including endocytosis activity and viability.

39

40 **TWEET** A new protocol describes a microfluidics-based assay for high-throughput interrogation of  
41 protein secretion kinetics in single cells. @BIOASTER @EyerFira @ETH\_DCHAB

42

43 **COVER TEASER** Microfluidics-based analysis of protein secretion

44

45 **Up to three primary research articles where the protocol has been used and/or developed.**

46 1. Eyer, K., Doineau, R. C. L., Castrillon, C. E., Briseño-Roa, L., Menrath, V., Mottet, G., et al.  
47 (2017). Single-cell deep phenotyping of IgG-secreting cells for high-resolution immune  
48 monitoring. *Nature Biotechnology*, 35(10), 977–982. <http://doi.org/10.1038/nbt.3964>

49

50 **ABSTRACT**

51 Characterization of immune responses is currently hampered by the lack of systems allowing  
52 quantitative and dynamic phenotypic characterization of individual cells, and especially analysis of  
53 secreted proteins such as cytokines and antibodies. We recently developed a simple and robust  
54 microfluidic platform, DropMap, to measure simultaneously the kinetics of secretion and other  
55 cellular characteristics, including endocytosis activity, viability and expression of cell-surface markers,  
56 from tens of thousands of single immune cells. Single cells are compartmentalized in 50 pL droplets  
57 and analyzed using fluorescence microscopy combined with an immunoassay based on fluorescence  
58 relocation to paramagnetic nanoparticles aligned to form beadlines in a magnetic field. The protocol  
59 typically takes 8-10 hours after preparations of microfluidic chips and chambers, which can be  
60 prepared in advance. In contrast, enzyme-linked immunospot (ELISPOT), flow cytometry, time of  
61 flight mass cytometry (CyTOF), and single-cell sequencing only allow end-point measurements, and  
62 do not allow direct, quantitative measurement of secreted proteins. We illustrate how this system  
63 can be used to profile downregulation of tumor necrosis factor- $\alpha$  (TNF- $\alpha$ ) secretion by single  
64 monocytes in septic shock patients, and to study immune responses by measuring rates of cytokine  
65 secretion from single T cells and to measure affinity of antibodies secreted by single B cells.

66

67

68 **Introduction**

69 The last few years have seen rapid progress of single-cell sequencing technologies in both  
70 fundamental and clinical research<sup>1-3</sup>. Single-cell RNA sequencing (scRNA-seq), in particular, is proving  
71 to be a powerful tool to study gene expression at the single-cell level and to characterize cell-type  
72 diversity<sup>4</sup>. Although methods such as droplet-based scRNA-seq<sup>5</sup> enable high-throughput analysis of  
73 tens-of-thousands of individual cells, measuring transcriptional profiles is not sufficient to fully  
74 understand cellular activity, as protein concentration and subcellular localization cannot be reliably  
75 inferred from mRNA expression levels<sup>6, 7</sup>. As proteins are implicated in most biological functions,  
76 numerous approaches have been developed to assess protein expression at the single-cell level. In  
77 particular, fluorescence-based flow cytometry<sup>8</sup> and time of flight mass cytometry (CyTOF)<sup>9</sup>, which  
78 allow medium to high-throughput single-cell phenotyping based on the detection of intracellular and  
79 cell-surface proteins, but not secreted proteins. The inability to directly detect secreted proteins can  
80 be partially alleviated using experimental strategies such as blockage of secretion pathways<sup>10, 11</sup>, but  
81 it is neither possible to tell whether the protein is secreted or stored intracellularly, nor to measure  
82 secretion rates. Fluorescence microscopy and flow cytometry allow reliable simultaneous analysis of  
83 6-10 distinct markers, while CyTOF allows simultaneous detection of as many as 40 markers<sup>9, 12,13</sup>.  
84 Recently, droplet-based single-cell sequencing techniques have also been developed to quantify cell-  
85 surface proteins using antibodies labeled with oligonucleotides<sup>7, 14, 15</sup> (rather than fluorescence or  
86 mass tags), which allows simultaneous analysis of the transcriptome of the same cell<sup>7, 14</sup>. In contrast,  
87 enzyme-linked immunospot (ELISPOT)<sup>16</sup> has been used extensively to detect proteins secreted from  
88 individual cells. Although simple to implement, this technique is poorly quantitative. ELISPOT assays  
89 can be used to determine the frequency of secreting cells but, even then, discrimination between  
90 signals due to secretion and background staining can be difficult<sup>17, 18</sup>. Importantly, ELISPOT, flow  
91 cytometry, CyTOF, and single-cell sequencing are all only based on end-point measurements, which  
92 do not reflect the dynamic nature of cellular behavior.

93 There is, hence, a need for quantitative high-throughput systems that allow dynamic single-cell  
94 phenotyping, including detection of secretion rates and binding activities of both cell-surface and  
95 secreted proteins. This information is crucial for the accurate analysis of immune responses that are  
96 mediated by both cell-membrane receptors and secretion of soluble factors, notably antibodies,  
97 chemokines and cytokines<sup>19</sup>. Deciphering dynamic processes at the single-cell level is critical to  
98 describe and understand the fundamental mechanisms underlying immunity, to develop new and  
99 improved strategies for vaccination and cancer immunotherapy, and to diagnose and treat  
100 inflammatory, autoimmune and infectious diseases.

101 Recently, novel technologies, based on microfabrication and microfluidics, have been developed to  
102 analyze the secretome of individual cells<sup>20-31</sup>, some of which have been used to measure the  
103 secretion of multiple cytokines and to detect antibody secretion and antigen binding<sup>30, 31</sup>.  
104 Compartmentalization of individual cells in picoliter volume droplets in microfluidic systems<sup>32, 33</sup> has  
105 also been used for high-throughput screening and sorting of antibody-secreting cells based on the  
106 binding or inhibitory activity of secreted antibodies<sup>34-36</sup> and to analyze cellular heterogeneity in  
107 cytokine-secreting immune cells<sup>37</sup>. Although promising, these assays are only based on endpoint data  
108 and do not reflect the dynamic expression of immune response.

109 To overcome these limitations, we have recently described a simple and robust droplet microfluidic  
110 method, DropMap (Fig. 1), which we used to study the humoral immune response in mice  
111 immunized with tetanus toxoid<sup>38</sup>. With DropMap, single IgG-secreting cells are compartmentalized in  
112 tens of thousands of 50 pL droplets to form a stationary two-dimensional droplet array allowing  
113 kinetic analysis by optical microscopy. A fast and ultrasensitive in-droplet immunoassay, based on  
114 fluorescence relocation to paramagnetic nanoparticles that are aligned to form beadlines in a  
115 magnetic field, allows simultaneous measurement of the IgG secretion rate and affinity for thousands  
116 of single cells in parallel. In our study, we discovered that immunization results in dramatic increases  
117 in the range of both single-cell secretion rates and IgG affinities, which spanned at maximum 3 and 4  
118 logs, respectively<sup>38</sup>. We also showed differences in dynamics of secretion rates and affinities of IgGs  
119 within and between spleen and bone marrow<sup>38</sup>.

120  
121 Here we present a detailed step-by-step protocol for the DropMap system, and describe how the  
122 system can be extended to study a range of different immune cells, including B cells, T cells and  
123 monocytes, and to analyze the secretion of a variety of different proteins, such as different antibody  
124 isotypes, and a variety of murine and human cytokines (including TNF- $\alpha$ , IFN- $\gamma$ ; IL-2 and IL-6). We also  
125 describe how the measurement of secretion can be combined with the measurement of other  
126 parameters, including affinities of secreted antibodies, expression of cell-surface markers,  
127 endocytosis and cell viability. The method is rapid and sensitive, enabling, for example, the detection  
128 of secreted proteins from a single cells in as little as 30 min, compared to generally more than 6  
129 hours for conventional single-cell assays such as ELISPOT<sup>16</sup>. It is a flexible system to analyze humoral,  
130 cellular and innate immune responses. To illustrate the performance of DropMap, we describe its  
131 applications to immune responses analyses in a murine immunization model by measuring secretion  
132 rate and affinity of antibodies secreted by single B cells. Importantly, from a clinical standpoint, we  
133 also reveal the downregulation profiles of TNF- $\alpha$  secretion by single monocytes obtained from septic  
134 shock patients.

135

136 **Comparison with other methods**

137 ELISPOT, flow cytometry, CyTOF, and scRNA-seq are all based on endpoint measurements, which is  
138 advantageous for throughput but does not reflect the dynamic nature of cellular behavior. They do  
139 not allow the quantitative characterization of secreted proteins by living cells. Recently, commercially  
140 available technologies based on compartmentalizing cells in microfabricated chambers have been  
141 developed to perform a range of assays, including real-time IgG and cytokine secretion, apoptosis  
142 and cell-cell interaction<sup>39-41</sup>. For example, the Berkeley Lights system allows optofluidic handling and  
143 analysis of single cells, including recovery of individual cells for sequence analysis, but can analyze  
144 ~10,000 cells as the system currently has 14115 chambers (“nanopens”), whereas the DropMap  
145 system can currently analyze up to 300,000 cells. Furthermore, when used to analyze antibody  
146 secretion, the Berkeley Lights system only provide a binary (yes/no) result<sup>41</sup>, whereas, DropMap  
147 enable simultaneous determination of both antibody secretion rate and affinity.

148 Other technologies using droplet microfluidics have been developed for high-throughput, single-cell,  
149 protein secretion measurement<sup>35, 37, 42, 43</sup>. However, as previously mentioned, these are endpoint  
150 approaches, and do not assess the dynamic nature of single-cell secretome. Droplet microfluidics has  
151 also been used for real-time measurement of T cell activation upon recognition of target tumor cells  
152 Segaliny *et al.* However, the number of droplets containing T cells and target cancer cells was low  
153 (due to Poisson statistics of cell encapsulation)<sup>44</sup>.

154 DropMap, in contrast, allows the direct measurement of protein secretion by individual living cells  
155 and the quantitative assessment of secreted proteins. Hence, using DropMap, the dynamic behavior  
156 of single-cells can be measured over time, allowing, for example, the direct and quantitative  
157 assessment of secretion rates of proteins such as antibodies, cytokines and chemokines, and, in the  
158 case of antibodies, DropMap enables simultaneous determination of both antibody secretion rate  
159 and affinity. A DropMap chamber surface of 1 cm<sup>2</sup> allows the observation and analysis of 60,000  
160 droplets: i.e. around 20,000 cells over up to 12 hours. Currently, the maximum number of cells we  
161 have detected simultaneously with DropMap is around 300,000 cells with a time resolution around  
162 21 minutes. The number of eukaryotic cells that can be analyzed is therefore similar to the number  
163 that can be analyzed by scRNA-seq (~ 10<sup>5</sup>), ELISPOT (~10<sup>5</sup> per well) and using microfabricated  
164 nanowells (~10<sup>5</sup>), but less than can be analyzed using flow cytometry (~10<sup>8</sup>) CyTOF (~10<sup>7</sup>) or droplet  
165 microfluidics with in-flow detection, where, using a similar magnetic beadline-based immunoassay,  
166 as many as 2.5 million eukaryotic cells can be analyzed per experiment<sup>45</sup>. The maximum number  
167 of markers that can currently be detected simultaneously with DropMap is 4, as described herein,  
168 but it should be possible to extend this to 6-10 markers, as for the other systems based on  
169 epifluorescence microscopy. The use, in DropMap, of an assay based on fluorescence relocation also  
170 negates the need for washing within the protocol.

171

172 **Protocol limitations**

173 Our protocol inherits the generic limitations of closed homogenous fluorescence-based assays. Once  
174 immobilized, nothing can be added or extracted from the droplets without losing their identity (as  
175 defined by their position). Therefore, the immunoassay cannot be washed, no enzymes can be used  
176 for signal amplification, and multi-step assays are not possible. The immunoassays sensitivity and  
177 range is defined by the number of added nanoparticles and detection reagent, therefore care should  
178 be taken when adapting the sensitivity and range of the assay to prevent excess false-positive or  
179 negative results (see also Box 1 and 2).

180 The biggest drawback of the protocol is the need for a known analyte of interest, since in the  
181 sandwich immunoassays the antibody pair is chosen according to the analyte, and the performance  
182 of the assay depends critically on the affinity and specificity of the antibodies. Also, when assaying  
183 secreted antibodies, since purified antigens are used in the assays, cross-reactivities or unspecific off-  
184 target binding of the antibodies are not taken into account and need to be characterized using other  
185 methods.

186 Due to the need for imaging in different fluorescent channels, care should be taken regarding optical  
187 phenomena such as pixel saturation, photo-bleaching or spectral overlap. This overlap also limits the  
188 number of readouts that could be used to probe several cellular functions within the droplets, thus  
189 reducing the multiplexing capability when compared to CYTOF or single-cell sequencing.

190 Long-term studies over days are also limited due to the inability to add fresh nutrients to the cells  
191 without losing their identity. Therefore, the longest experimental time is defined by the  
192 disappearance of a crucial nutrient, or the accumulation of waste products in the droplets. This  
193 depends on the nature of the cells analyzed, but using mammalian cells (Chinese hamster ovary, CHO  
194 cells), the longest assay we have performed is 12 hours. The frequency of dead cells (stained with  
195 propidium iodine) encapsulated in droplets was not significantly different from the reference culture  
196 in a standard CO<sub>2</sub> incubator over 12 hours of incubation time ( $3.2 \pm 1.6 \%$  and  $2.6 \pm 1.6 \%$ , for  
197 droplets and the reference culture respectively. N = 3, two-tailed unpaired t test p = 0.67).

198

199 **Expertise needed to perform the protocol**

200 A competent graduate student or post-doc can perform the protocol. There are two crucial parts of  
201 the protocol. First, the extraction and preparation of the biological sample, i.e. the cells, is of great  
202 importance. These should be extracted and prepared with the least stress possible since even minor  
203 changes in the protocol might result in lower secretion rates, and therefore variations in the results.



204 The work with human and animal samples needs to be performed by properly trained and skilled  
205 experimenters, with appropriate safety precautions, with ethical approval where necessary, and in  
206 accordance with local legislation. Second, the proper preparation of the chamber and droplets is of  
207 high importance to eliminate or restrict droplet movement over time and improve data quality and  
208 reliability of the process, but a researcher from any discipline easily masters the procedure.

209

## 210 **Experimental design**

211 The DropMap protocol is based on compartmentalizing single cells in tens of thousands of 50 pL  
212 droplets that are immobilized in two-dimensional droplet arrays and analysed by fluorescence  
213 microscopy<sup>38</sup> (Fig.1). The droplets can be therefore monitored over time and cellular dynamics are  
214 captured by taking images at regular intervals. Compartmentalization of single cells in droplets allows  
215 the measurement of secreted molecules which remain in the droplets, in combination with  
216 measurements of cell-surface markers and other phenotypic characteristics. Secreted molecules are  
217 quantified using a fluorescence relocation-based, sandwich immunoassay. The analytes are captured  
218 on antibody-coated paramagnetic nanoparticles in the droplets using a capture antibody. These  
219 nanoparticles are aligned to form a beadline by applying a magnetic field, and the captured analytes  
220 are quantified by measuring relocation of a fluorescently-labelled detection antibody to the beadline.  
221 The protocol consists of six major stages:

222 **Microfabrication of the droplet production chip (Steps 1-22).** Microfluidic chips for droplet  
223 production are fabricated in poly(dimethylsiloxane) (PDMS) using soft-lithography<sup>46</sup> as described  
224 previously<sup>35</sup>. Droplet-makers are also commercially available from a variety of commercial suppliers  
225 for laboratories without the necessary equipment and facilities to perform these steps. The droplet  
226 production chip is designed to produce monodisperse 50 pL droplets using hydrodynamic flow  
227 focusing<sup>47</sup> and contains three inlets to introduce, respectively, (i) the fluorinated carrier oil containing  
228 fluorosurfactant, (ii) the suspension of cells and (iii) the assay reagents (functionalized nanobeads,  
229 labelled detection probes, a live/dead cell probe, and others), as well as one outlet for collecting the  
230 produced droplets<sup>35</sup> (Fig. 1 and see Supplementary Data 1 for the complete chip design - CAD file).

231 **Microfabrication of the droplet incubation chamber (Steps 23-30).** The immobilization and storage  
232 of aqueous droplets in a 2D array is the core of the DropMap approach. Immobilization of the  
233 droplets allows for time-course measurements of droplet-based biological assays<sup>48-53</sup>. Due to the  
234 height of the chamber being less than the droplet diameter, the observation chamber is able to  
235 immobilize 50 pL droplets. Incubations and observations over time are therefore made possible for  
236 short to medium time ranges (5 min to < 24h) at temperatures between 4°C and 37 °C.

237 We use a simple, cost-effective and reproducible method based on double-sided tape and two  
238 standard microscope slides (75 mm x 25 mm x 1 mm) to fabricate the droplet incubation device (Fig.  
239 2, see Supplementary Data 2 and 3 for the mask for the double-sided tape to prepare the  
240 observation chamber and the mask for laser ablation). The fabrication method is flexible and  
241 customized microfluidic chambers can be fabricated depending on the droplet volume and the  
242 number of droplets to be analyzed: several double-sided adhesive tapes with different thicknesses  
243 are commercially available (for example from 3M) and any observation chamber shape and size can  
244 be made by cutting the tape using a plotter. The use of glass results in an optically transparent  
245 system, whilst the double-sided tapes used adheres strongly and stably to the glass surfaces  
246 preventing fluid leakage and evaporation. Lastly, after the experiments the chamber can be cleaned  
247 and reused several times. To do so, the outer surfaces are cleaned with ethanol or isopropanol and  
248 the chamber flushed with pure fluorinated oil to remove droplets.

249 **Functionalization of nanoparticles (Steps 31A-31B).** Another important key feature of our droplet-  
250 based immunoassay is the use of many paramagnetic nanoparticles per droplet (see also Box 3).  
251 Magnetic nanoparticles are well-suited to immunodetection technologies owing to their large  
252 surface-to-volume ratio, monodispersity, stability and easy manipulation in a magnetic field.  
253 Compared to approaches relying on the co-encapsulation of a single cell and a single microparticle<sup>35</sup>,  
254 the use of nanoparticles increases the binding capacity and lowers the number of droplets containing  
255 no particles, which improved the performance of the assay. The protocol was optimized so that, once  
256 a strong magnetic field is applied, each droplet contains a single, homogeneous, elongated aggregate  
257 of hundreds of nanoparticles, which appears in the bright-field images as a horizontal dark beadline  
258 located in the droplet (Fig. 1, 3). The number of nanoparticles per droplet defines the capacity of the  
259 immunoassay, and can be adjusted to the expected secretion rates to allow optimal results.  
260 However, a certain minimum (100-200 beads/droplet) is needed to form a measurable beadline.

261 Secreted molecules are captured onto paramagnetic nanoparticles for detection, typically *via* capture  
262 antibodies. The immobilization of capture antibodies onto the nanoparticles is a crucial step for the  
263 success of the protocol<sup>54-59</sup>. The performance of antibody-based biosensors is directly related to the  
264 orientation of antibodies on the nanoparticles and accessibility of the paratope that binds the  
265 targeted analyte. In this protocol, we describe the use of two targeted coupling strategies. First, we  
266 describe a boronic acid (BA)-based coupling strategy for precise orientation of capture antibodies on  
267 the surface of magnetic nanoparticles<sup>54, 60-62</sup> (Fig. 3a-c) and second, a strategy based on biotinylated  
268 capture antibodies coupled to streptavidin-coated nanoparticles (Fig. 3d-f).

269 **Automated image acquisition (Steps 38-45).** To perform imaging, the microfluidic chamber is placed  
270 on a motorized stage of an inverted epifluorescence microscope. In our case, 10X magnification was  
271 used as a compromise between scanning time and resolution for object detection within each  
272 droplet. We image between 75-225 fields of view in multiple channels (up to five, depending on the  
273 integrated assays): 75 fields of view (135 mm<sup>2</sup>) results in around 60,000 imaged droplets; i.e. 10-  
274 20,000 cells. Throughput can be improved by increasing the imaged area. However, when scanning  
275 large areas of a sample with high resolution, scanning time as well as processing time (of large  
276 amount of imaging data) can become limiting steps for the throughput of the procedure. Here,  
277 binning of pixels during acquisition may help to solve some of these issues.

278 As both automated object detection and fluorescence intensity measurements rely on focus quality,  
279 control of focus drift throughout the imaging procedure (of a large area over long times) is crucial.  
280 Mechanical effects, vibrations, thermal changes and droplets movement can cause the focus to drift.  
281 We addressed this limitation by using the Perfect Focus System (PFS) of the Nikon microscope, but  
282 other microscopes might offer similar solutions.

283

284 **Cell preparation, encapsulation and incubation in droplets (Steps 46A-46B).** This analytical system is  
285 suitable for many different cells from various tissues and species. Primary cells are sensitive and  
286 fragile, therefore requiring gentle handling during extraction and manipulation. Due to the  
287 quantitative nature of the measurements described in this protocol, even small deviations might  
288 result in significant differences. Gentle handling and rapid extraction of cells is important, and for  
289 optimal results, the cells should be present as a singularized suspension. Before encapsulation, the  
290 cell density needs to be adjusted so that the frequency of droplets containing a single cell is  
291 maximized, while minimizing the frequency of droplets containing multiple cells (see Box 3)<sup>35</sup>.

292 Compartmentalization of cells in droplets will further affect cell survival. The surfactant is a key  
293 reagent for the droplet assays<sup>35, 63</sup>: it must be non-cytotoxic, and must stabilize droplet interfaces and  
294 prevent the coalescence of droplets during incubation. The use of the nonionic perfluoro-polyether  
295 fluorosurfactant (600 g/mol PEPE tails and 2000 g/mol heads)<sup>35</sup> in combination with fluorinated  
296 carrier oils such as HFE-7500 (3M) is recommended. At some point, nutrient depletion and pH  
297 changes will be a limiting factor for long-term studies of the encapsulated cells. The in-droplet pH is  
298 maintained by the addition of HEPES<sup>64</sup>, and the fluorinated oil, which can dissolve ~20 times more  
299 oxygen than water<sup>65</sup>, used as a continuous phase, additionally serves as an, albeit limited, oxygen  
300 reservoir<sup>66, 67</sup>. In addition, as fluorinated oils are very poor solvents for non-fluorinated molecules<sup>68, 69</sup>  
301 they are well suited for cell-based and biochemical assays. Various biocompatible fluorinated oils and

302 fluorosurfactants can be ordered from a large number of suppliers such as 3M, RAN Biotechnologies,  
303 Dolomite, Sphere Fluidics and Bio-Rad. We confirmed the survival of primary monocytes over a 12-  
304 hour time span, and the survival of primary murine splenocytes over the same time-period in 50  $\mu$ L  
305 droplets. Furthermore, we added in our protocol a simple and sensitive cytotoxicity assay to  
306 discriminate dead and live cells to exclude any signals that might stem from dead or dying cells.

307 **Image processing (Steps 47A-47B).** We developed a robust, custom-made Matlab-based software to  
308 detect and, if necessary, track droplets in time-lapse image sequences and monitor the status of their  
309 content over time. The software analyses the images over time in different fluorescence and bright  
310 field channels. First, the droplets are detected in bright field images using an algorithm that detects  
311 circles of a given diameter. In a next step, a binary mask of the detected droplets is generated, and  
312 this mask is overlaid onto the following fluorescence images to analyze each droplet separately.  
313 Within each droplet, the software measures the fluorescence of droplets, cells and beadlines (Fig. 4).

314 The software output is a spreadsheet containing morphological and fluorescence intensity  
315 parameters for different intra-droplet objects or regions over time. All measured fluorescence  
316 intensities on objects (i.e. magnetic beadline, cell or whole droplet) are normalized by the  
317 background fluorescence of the droplet in order to compensate locally for potential heterogeneity of  
318 illumination of the field, increase the sensitivity (signal-to-noise ratio is more differentiating than the  
319 raw beadline signal), and reduce the impact of photobleaching on results.

320

321 **Materials**

322 **Biological materials**

- 323 • Human blood ! **CAUTION** Experiments using human blood samples must conform to the  
324 relevant Institutional and National regulations and requires informed consent from all  
325 participants. See just below for the permissions obtained for the use of human blood for this  
326 Protocol:
- 327 - Samples from septic shock patients (Table 1) were obtained from the prospective cohort  
328 MICROFLU-SEPSIS which has been approved by the French Ethical Committee CPP Sud  
329 Ouest et Outre Mer 4 (registration number 2017-A01134-49). Patients were included in  
330 the medical intensive care unit of Cochin hospital and informed consent was obtained  
331 from all the participants or their legally authorized representatives.
  - 332 - For sepsis application, blood sample collection from healthy donors was performed  
333 according to the Ethical Committee of the Investigation Clinique et Acces aux Ressources  
334 Biologiques (ICAReB) platform (Dr Marie-Noelle Ungeheuer, Centre de Recherche  
335 Translationnelle, Institut Pasteur, Paris, France) as part of the DIAGMICOLL or  
336 CoSImmGen (N° CORC: 2008-16 and 201-06) protocol, which has been approved by the  
337 French Ethical Committee (CPP), Ile-de-France. Informed consent was obtained from all  
338 donors (Table 1).
  - 339 - For cytokine-secreting T-cells application, Peripheral Human blood was also collected  
340 from healthy patients at the "Etablissement Français du Sang". Donors were recruited  
341 after a medical selection process complying with French regulations, and they gave their  
342 informed consent to participation in the study.
- 343
- 344 • Mouse spleen and bone marrow. In this protocol, we used *Mus musculus*, BALB/cJrj,  
345 females, age 8-10 weeks at the start of the immunization, supplied by Janvier Laboratories. !  
346 **CAUTION** Experiments using animal samples must conform to the relevant Institutional and  
347 National regulations. In this work, the mice experiments have been validated by the CETEA  
348 ethics committee number 89 (Institute Pasteur, Paris, France) under #2013-0103, and by the  
349 French Ministry of Research under agreement #00513.02, and were part of larger scientific  
350 study.
- 351
- 352

	<b>Gender</b>	<b>Age</b>	<b>Sepsis source</b>	<b>SOFA<sup>#</sup></b>
<b>Septic Patient 1</b>	Male	61	Cutaneous	8
<b>Septic Patient 2</b>	Female	88	Urinary tract	6

<b>Septic Patient 3</b>	Female	63	Osteo-articular	8
<b>Healthy Donor 1</b>	Male	47	ND	ND
<b>Healthy Donor 2</b>	Female	42	ND	ND
<b>Healthy Donor 3</b>	Female	35	ND	ND

353

354

355

356

357

358

- **Table 1. Characteristics of healthy donors and septic patients at admission in the intensive care unit.** Gender, age, sepsis source and SOFA score. The SOFA (Sequential Organ Failure Assessment) score is a bedside applicable score designed to score organ dysfunction with less focus on mortality prediction.

### 359 Reagents -

360 **CAUTION** Wear appropriate protective clothing and equipment when manipulating chemical and  
361 biological reagents.

362

363

364

365

366

367

368

369

370

371

372

373

374

375

- Ultrapure DNase/RNase-free distilled water (Invitrogen, cat. no.10977049).
- Isopropanol (VWR 208224321). ! **CAUTION** Isopropanol liquid and vapor is highly flammable. Handle away from ignition sources and fire.
- Acetone (VWR 322201). ! **CAUTION** Acetone liquid and vapor is highly flammable. Handle away from ignition sources and fire.
- Ethanol (VWR 208224321). ! **CAUTION** Ethanol liquid and vapor is highly flammable. Handle away from ignition sources and fire.
- 1H, 1H, 2H, 2H-Perfluorododecyltrichlorosilane (Sigma-Aldrich, cat. no. 729965)! **CAUTION** This reagent is corrosive and moisture sensitive. Work in a fume hood to avoid inhalation of silane.
- HFE-7500 (3M, cat. no. 98-0212-2928-5)! **CAUTION** Avoid direct contact with this liquid, as it may cause respiratory, skin and eye irritation.
- Fluorinated surfactant (Ran Biotechnologies, cat. no 008).
- Poly(dimethyl siloxane) (PDMS) and curing agent (Dow Corning, Sylgard 184).

### 376 Application sepsis

377

378

379

380

381

382

383

384

- Bovine Serum Albumin (BSA) (Sigma-Aldrich, cat. no A7960).
- Roswell Park Memorial Institute (RPMI) 1640 Medium (PanBiotech, cat. no. P04-17500).
- Phosphate Buffered Saline (PBS) (Dominique Dutscher, cat. no. L0612-500).
- Penicillin-streptomycin (Life Technologies, cat. no. 15140-122).
- HEPES (Dominique Dutscher, cat. no. L0180-100).
- Fetal Bovine Serum (FBS) (HyClone cat. no. SH30070.03).
- Anti-CD14, blue violet conjugate (Clone TÜK4) (Miltenyi Biotec Cat# 130-094-364, RRID:AB\_10831023), Lot# 5171130409.

- 385 • Capture anti-TNF- $\alpha$  antibody (Antibody TNF5) ([MABTECH Cat# 3510-6-1000](#),
- 386 [RRID:AB\\_907379](#)), Lot#16, non-biotinylated).
- 387 • Detection PE-anti-TNF- $\alpha$  antibody Clone: cA2 ([Miltenyi Biotec Cat# 130-120-489 without](#)
- 388 [azide Cat#120-014-229](#), [RRID:AB\\_2752115](#)), Lot#5160222264.
- 389 • Recombinant TNF- $\alpha$  protein (Biolegend, cat. no. 570108).
- 390 • NucView488 (Biotium, cat. no. 99949).
- 391 • MitoView633 (Biotium, cat. no. 99950).
- 392 • LPS (Sigma-Aldrich, cat. no. L2637, 3012 and 3137).
- 393 • Dextran 20 % (wt/wt), 500 kDa (Sigma-Aldrich, cat. no. D8802).
- 394 • 300 nm dimeter Carboxyl Adembeads (Ademtech, cat. no 2131).
- 395 • EDC (Thermo Fisher Scientific, cat. no. 77149). ! **CRITICAL** This material is moisture sensitive.
- 396 Upon receipt, make aliquots and store them at -20°C.
- 397 • SulfoNHS (Thermo Fisher Scientific, cat. no 24510). ! **CRITICAL** This material is moisture
- 398 sensitive. Upon receipt, store at 4°C.
- 399 • Ethanolamine (Sigma-Aldrich, cat. no E9508). ! **CAUTION** This material is irritant. Work in a
- 400 fume hood.
- 401 • 10 X Activation buffer 10X for Carboxyl-Adembeads Coupling (Ademtech, cat. no 10101)
- 402 • 10 X Storage Buffer 10X (Ademtech, cat. no 10201)
- 403 • 3-aminophenylboronic Acid (Sigma, cat. no A71751)
- 404 • EasySep Direct Human Monocyte isolation Kit (STEMCELL Technology, cat. no 19669).

#### 405 **Application murine IgG-secreting cells**

- 406 • Knockout Serum Replacement (Thermo Fisher Scientific, cat. no. 1082808).
- 407 • Human Serum Albumin (rHSA), recombinant (SigmaAldrich, cat. no. A9731).
- 408 • HEPES (ThermoFisher, cat. no. 15630080).
- 409 • DPBS (ThermoFisher, cat. no. 14190250).
- 410 • Penicillin-streptomycin (Life Technologies, cat. no. 15140-122).
- 411 • Pluronic F-68, 10% (wt/vol) sterile filtered solution (Thermo Fisher Scientific, cat. no.
- 412 24040032).
- 413 • Pluronic F-127, 10% (wt/vol) sterile filtered solution (Thermo Fisher Scientific, cat. no.
- 414 P6866).
- 415 • RPMI 1640 Medium without phenol red (ThermoFisher, cat. no. 11835030).
- 416 • 300 nm diameter Bio-Adembeads Streptavidin plus (Ademtech, cat. no. 03132).
- 417 • CaptureSelect™ Biotin Anti-LC-kappa (Murine) Conjugate (ThermoFisher Scientific, cat. no.
- 418 7103152100), Lot#160707-02.
- 419 • AffiniPure F(ab')<sub>2</sub> Fragment Rabbit Anti-Mouse IgG, Fc $\gamma$  fragment specific ([Jackson](#)
- 420 [ImmunoResearch Labs Cat# 315-606-047](#), [RRID:AB\\_2340252](#)), Lot#103179.
- 421 • CellTrace™ Violet Cell Proliferation Kit (ThermoFisher Scientific, cat. no. C34557).
- 422 • Zenon™ Alexa Fluor™ 488 Mouse IgG2b Labeling Kit ([Thermo Fisher Scientific Cat# Z25202](#),
- 423 [RRID:AB\\_2736943](#)), Lot#1450052 .

#### 424 **Application cytokine-secreting T-cells**

- 425 • IFN gamma Monoclonal Antibody (MD-1) (Thermo Fisher Scientific Cat# 14-7317-85,
- 426 RRID:AB 468474), Lot#4295084, biotinylated in house.
- 427 • IFN gamma Monoclonal Antibody (clone 4S.B3), APC conjugate (Thermo Fisher Scientific Cat#
- 428 17-7319-82, RRID:AB 469506), Lot#4281150.
- 429 • TNF alpha Monoclonal Antibody (MAb1) (Thermo Fisher Scientific Cat# 14-7348-85,
- 430 RRID:AB 468488), Lot#E05529-432, biotinylated in house.
- 431 • TNF alpha Monoclonal Antibody (MAb11), PE conjugate (Thermo Fisher Scientific Cat# 12-
- 432 7349-81, RRID:AB 466207), Lot#4290466.
- 433 • IL-2 Polyclonal Antibody, Biotin (Thermo Fisher Scientific Cat# 13-7028-81, RRID:AB 466900),
- 434 Lot#4307122 and 2049448.
- 435 • IL-2 rabbit anti-human (PeptoTech Cat# 500-P22-100ug, RRID:AB 147898), Lot#0204CY12RB,
- 436 labelled in house with Alexa 555
- 437 • IL-4 Monoclonal Antibody (MP4-25D2), Biotin conjugate (Thermo Fisher Scientific Cat# 13-
- 438 7048-81, RRID:AB 466904), Lot#1963900.
- 439 • IL-4 Monoclonal Antibody (8D4-8), APC conjugate, (Thermo Fisher Scientific Cat# 17-7049-81,
- 440 RRID:AB 469497), Lot#4275080.
- 441 • Anti-human CD3, clone HIT3a, Alexa Fluor® 647 conjugate (BioLegend Cat# 300322,
- 442 RRID:AB 493693), Lot#RT2101610.

443

#### 444 **EQUIPMENT –**

##### 445 **General lab equipment**

- 446 • Gloves (Crolex powder-free nitrile).
- 447 • Microscope slides, frosted ground-edges (VWR, cat. no. 63115553).
- 448 • Ultraviolet curing adhesive (Nurland optical adhesive, cat. no.68 P/N 6801).
- 449 • Disposable slide for cell counting: Fast Reader 102 (Dominique Dutscher, cat. no. 390498).
- 450 • Reusable biopsy punch diameter 0.75 mm and 6 mm (WPI, cat. no. 504529 and 504532).
- 451 • Sterican needles 23 G for 0.56 mm diameter microtubing (Braun, cat no; 921021).
- 452 • Sterican needles 27 G for 0.30mm diameter microtubing (Braun, cat no. 921018).
- 453 • PTFE microtubing (0.56 × 1.07 mm; Fisher Scientific, cat. no. 1192-9445).
- 454 • PTFE microtubing (0.30 × 0.76 mm; Fisher Scientific, cat. no. 1191-9445).
- 455 • Sterile 1 ml syringes (Braun Omnifix, cat. no. 9204512).
- 456 • Sterile low binding microcentrifuge tubes (Dominique Dutscher, cat.no 27210).
- 457 • Petri dishes (100 mm diameter × 15 mm; BD Falcon, cat. no. 351029).
- 458 • Nanoport 6-32 (Cil , cat no N-126-01).
- 459 • Cap (Cil, cat no P-555).
- 460 • MicroTight fittings (Cil, cat no P126S).
- 461 • Three low pressure syringe pumps neMESYS 290N, and control module Base 120 (both
- 462 Cetoni).
- 463 • Vortex LMS (Dominique Dutscher, cat. no 079030).



- 464 • Adjustable 2.5, 10, 20, 200 and 1,000 µl pipettes and sterile pipette tips (Eppendorf, cat no.:  
465 3123000012; 3123000020; 3123000039; 3123000055; 3123000063).
- 466 • 2.5, 10, 20, 200 and 1,000 µl sterile pipette tips ART (Thermo Fisher Scientific).
- 467 • Carousel holder for 6 micropipettes Research or 6 Multipettes (Dominique Dutscher, cat. no  
468 33076).
- 469 • Smart Spatula (Dominique Dutscher, cat.no. 059362).
- 470 • Centrifuge (Eppendorf 5810R and 5418R).
- 471 • Magnet holder for 1.5 microtube (Ademtech, cat. no 20101).
- 472 • EasySep Magnet (STEMCELL Technology, cat.no. 180001). ! **CAUTION** Strong magnetic field.  
473 Handle it carefully and keep it away from objects that respond to magnetic field.
- 474 • Falcon® Round-Bottom Polystyrene Tubes, 5 and 15 mL (Dominique Dutscher, cat. no.  
475 352051).
- 476 • Rapid-flow filter unit 0.2 µm-PES membrane 0.75 mm (Thermo Fisher Scientific, cat. no. 566-  
477 0020).
- 478 • Sonicator: Branson Model B200 ultrasonic cleaner (Dominique Dutscher, cat. no. 910586).
- 479 • Mini shaker vortex Lab Dancer (Dominique Dutscher, cat. no 250097).
- 480 • Rotating shaker SB3 Stuart (Dominique Dutscher, cat. no 250097).
- 481 • Drum 40 microtubes 1.5 mL (Dominique Dutscher, cat. no 90435).
- 482 • Inverted microscope for droplet generation (Olympus IX83).
- 483 • 96-well microtiter microplate (Greiner, cat.no. 650185).
- 484 • 96-well dark microtiter plate (Corning, cat.no 3991).
- 485 • Magnet holder for 96-well plate (Ademtech, cat. no 20106).
- 486 • Plate reader infinite M200 Pro (TECAN).

#### 487 **Chip fabrication**

- 488 • Disposable mixing cups (Dominique Dutscher, cat no 045108).
- 489 • Aluminum foil (Alupro, cat. no. A0626).
- 490 • Oven (Binder 300°C, Dominique Dutscher cat. no. 9010-0190).
- 491 • Vacuum desiccator (Sigma-Aldrich, cat. no D2672).
- 492 • Scalpel (Becton Dickinson, No. 11, cat. no. 371611).
- 493 • Oxygen plasma cleaner (Femto Science, Inc. CUTE.MRP).

#### 494 **Chamber fabrication**

- 495 • UV light source 5 (Opticure LED, Tech Optics Led, cat. no. 5090-200).
- 496 • Tweezers Dark blue forceps 111mm (Dutscher, cat no. 037876).
- 497 • CO<sub>2</sub> Laser (AxysLaser, C180 ii-CO<sub>2</sub>), or alternative method for drilling 1 mm holes in glass.
- 498 • Graphtec Cutting plotter CE6000-40 (Graphtec) or CAMEO plotter (Silhouette).
- 499 •

#### 500 **Chamber fabrication for sepsis application**

- 501 • Double-sided adhesive tape (Adhesive Research, cat. no. 92712).
- 502 • Binder clips (safe tool, cat no.: 8140.19; 8140.32).
- 503 • Magnet (FIRST4MAGNETS, cat. no. F75103). ! **CAUTION** These magnets are powerful. They
- 504 can be dangerous, handle them carefully. Keep it away from objects that respond to
- 505 magnetic field.
- 506 • Oven (Binder 300°C, Dominique Dutscher cat. no. 9010-0190).
- 507

#### 508 **Chamber fabrication for IgG application**

- 509 • Orafol Tape Series 1375 (Orafol, SDAG Adhésifs).
- 510 • Silicone paper (135 g/m<sup>2</sup>, SDAG Adhésifs). ! **NOTE** The Orafol 1375 is only covered on one
- 511 side with paper. Use this tape to cover the other side, and cut through this tape in the
- 512 assembly to generate optimal results for chamber fabrication.
- 513 • 2 Magnets (K&J Magnetics, cat. no. BZX082). ! **CAUTION** These magnets are powerful. They
- 514 can be dangerous, handle them carefully. Keep it away from objects that respond to
- 515 magnetic field.
- 516 • 3D printed holder for magnets (according to the Supplementary File 4)
- 517 • Thermopress capable of a pressing 7 bar and heating to 150 °C (Scamex).

#### 518 **Microscope and image acquisition**

- 519 • Inverted microscope for time-lapse imaging (Nikon, Eclipse Ti-2E):
- 520 • Digital CMOS camera (ORCA FLASH 4 LT, Hamamatsu); 2048(V) x 2048(H) pixel array with 6.5
- 521 x 6.5 μm<sup>2</sup> pixel size.
- 522 • Transmission light source (powerful white LED, pE-100wht, CoolLED). It replaces typical
- 523 100W halogen lamp.
- 524 • LED-based excitation light engine (Lumencor, SOLA SE II,).It replaces mercury arc lamp.
- 525 • 10x CFI Plan Apochromat Objective (Nikon, cat. no. MDR00105).
- 526 • Microscope enclosure and temperature controller (Oko-lab, cat. no. H201-T-UNIT-BL).
- 527 • Motorized xy stage (Nikon, cat no MECS MEC56110).
- 528 • Software for stage control and image acquisition (Nikon, cat no NIS-AR Log MQS3 1000).
- 529 • Perfect Focusing System 2 (PFS2, Nikon, cat. no. MEP59390). ! **CRITICAL**: Needed to retain
- 530 focus over large measurement areas.
- 531 • DAPI fluorescence cube (Nikon, cat. no. DAPI-5060C: Exc. 377/50 nm, Em. 447/60 nm, Cutoff
- 532 409 nm)
- 533 • GFP fluorescence cube (Nikon, cat. no. GFP-1828A: Exc. 482/18 nm, Em. 520/28 nm, Cutoff
- 534 495 nm)
- 535 • CY3 fluorescence cube (Nikon, cat. no. CY3-4040C: Exc. 531/40 nm, Em. 593/40 nm, Cutoff
- 536 562 nm)

- 537 • CY5 fluorescence cube (Nikon, cat. no. CY5-4040C: Exc. 628/40 nm, Em. 692/40 nm, Cutoff  
538 660 nm)

### 539 **Software and analysis workstation**

- 540 • MATLAB (MathWorks, version 2018a, Image processing toolbox, VLFeat open source library,  
541 <https://www.vlfeat.org/install-matlab.html>).
- 542 • MATLAB Image analysis workstation: 8 Virtual processors, 2.6GHz, RAM 64 GB.
- 543 • DropCell.exe (<https://doi.org/10.6084/m9.figshare.11336663.v1>). **CRITICAL** Before first use  
544 of the Matlab application, it will have to be installed on your computer. This is done  
545 automatically by running the provided MyAppInstaller\_web.exe. The same installer file will  
546 offer to download and install the required version 9.4 (R2018a) of the MATLAB Runtime, if  
547 not already installed on your machine. An example of input\_parameters.txt file as well as a  
548 readme\_dropcell.txt file will be automatically copied to the folder where you will choose to  
549 install the application. **CRITICAL** Read carefully the readme\_dropcell.txt before first use of  
550 DropCell.exe. It describes the installation procedure as well as the input images naming rules.  
551

### 552 **REAGENTS SETUP–**

#### 553 **SILANE Solution**

554 To prepare 1% (vol/vol) silane solution, dilute 10  $\mu$ l 1H, 1H, 2H, 2H-Perfluorododecyltrichlorosilane in  
555 990  $\mu$ l filtered HFE-7500 oil. This solution should be prepared immediately before use.

556 **! CAUTION** This solution is irritant and corrosive, work in a fume hood with appropriate materials.

557 **CRITICAL** Use this reagent immediately after preparation.

558

#### 559 **Coupling buffer for boronic-based functionalization**

560 Dilute activation buffer 10-fold in pure distilled water. This buffer should be freshly prepared before  
561 use.

562

#### 563 **Storage buffer for boronic-based functionalization**

564 Dilute storage buffer 10-fold in pure distilled water. This buffer should be freshly prepared before  
565 use.

566

#### 567 **Quenching buffer for boronic-based functionalization**

568 100 mM ethanolamine in PBS. This buffer should be freshly prepared before use

569 **! CAUTION** This solution is corrosive and irritating; work in a fume hood.

570 **CRITICAL** Use this reagent immediately after preparation. Do not store.

571

#### 572 **Blocking buffer for boronic-based functionalization**

573 Blocking buffer is 1% (vol/vol) Dextran. Dilute dextran 20% (wt/wt) 20-fold in pure distilled water to  
574 obtain 1% (vol/vol) blocking buffer. This solution can be stored at 4°C for up to 6 months.

575 **! CAUTION:** Dextran 20% (wt/wt) is viscous pipette this solution very slowly.

576

#### 577 **Cell buffer for sepsis application**

578 Heat the FBS at 56°C in a water bath for 35 minutes. Cool at room temperature (20-25°C) and filter  
579 the serum using rapid-flow filter unit of 0.2 µm-PES membrane. Make 50-ml aliquots and store at  
580 -20°C. After thawing, centrifuge the serum at 3000g for 10 minutes at room temperature to remove  
581 large debris. Supplement RPMI 1640 Glutamax with 10% heat-inactivated FBS (vol/vol), 5% Penicillin-  
582 streptomycin (vol/vol), and 20 mM HEPES. Store culture medium at 4 °C and use it within 2 weeks  
583 after preparation.

584

#### 585 **Blocking buffer murine IgG application**

586 5% (vol/vol) Pluronic F-68 in PBS, sterile. Can be stored at -20°C in small aliquots ready to use. For  
587 short term storage, store at 4°C for up to 4 weeks.

588

#### 589 **Cell buffer 1 IgG application**

590 RPMI 1640 with Glutamax (w/o phenol red) supplemented with 10% KnockOut Serum Replacement  
591 (vol/vol), 1x Penicillin-streptomycin, 0.1% Pluronic F-127 (vol/vol), rHSA 0.5% (wt/vol) and 25 mM  
592 HEPES. Aliquot cell buffer and freeze at -20°C. For short term storage, store at 4°C for up to 1 week.  
593 Up to 4 weeks are possible when working in a sterile environment.

594 **! CRITICAL:** The use of rHSA and the removal of all products from animal origin reduces assay  
595 background and increases sensitivity.

596

#### 597 **Immobilization reagent IgG application**

598 CaptureSelect™ Biotin Anti-LC-kappa (Murine) Conjugate (stock concentration 1 mg/ml), diluted 1 to  
599 5 (v/v) in PBS. Aliquot in 50 µl and store at -20°C. For short term storage, store at 4°C for up to 4  
600 weeks.

601

602

#### 603 **PROCEDURE**

#### 604 **Microfluidic device fabrication from existing molds. Timing 4 h**

605 **CRITICAL:** Follow the instructions reported by Mazutis and colleagues<sup>35</sup> to design microfluidic chips  
606 and fabricate the wafer mold (see Supplementary Data 1 for our wafer design). Ready-to-use wafer

607 molds can be obtained from various commercially suppliers, thus avoiding photo-lithography steps  
608 (not described here, see reference<sup>70</sup>). Furthermore, finished droplet makers can be obtained directly  
609 from a variety of commercial suppliers such as Dolomite, Elveflow and others, avoiding steps 1-22. If  
610 purchased, droplet makers should be capable of forming 50  $\mu$ L droplets. S

611 **1.** Place the wafer on a circular piece of aluminum foil (around 2 cm larger diameter than  
612 wafer). Form a cup around the mold.

613 **2.** Dust-off the wafer mold with compressed nitrogen or air.

614 **! CRITICAL STEP** Care should be taken to remove any dust that might form clumps in the channels.

615 **3.** Place the aluminum foil cup containing the mold in a petri dish.

616 **4.** Per wafer, pour 45 g of PDMS and 5 g of curing agent (9:1 PDMS/curing (wt/wt) agent ratio)  
617 in a disposable beaker, then vigorously mix with 1000  $\mu$ l pipette tip or plastic fork.

618 **CRITICAL STEP** Do not forget to add the curing agent; and mix generously. It is difficult to remove  
619 non- or semi-cured PDMS from the wafer mold.

620 **5.** Degas the PDMS-curing agent mixture using a vacuum chamber until all air bubbles are  
621 removed.

622 **6.** Slowly pour the degassed PDMS-curing agent mixture on top of the wafer from Step 3.

623 **7.** Put the Petri dish under vacuum again and degas the PDMS until no bubbles are visible. If  
624 bubbles persist, gently remove remaining bubbles with an air blower then cover the petri dish with  
625 lid to protect the PDMS from dust.

626 **8.** Bake the wafer mold-containing Petri dish in a drying oven at 65 °C for 90 to 120 min to  
627 harden the mixture.

628 **9.** Cool down to room temperature and carefully peel off the PDMS from the wafer using a  
629 scalpel. Clean the PDMS and wafer with clean nitrogen or air.

630 **CRITICAL STEP** The wafer is very fragile, any excessive pressure or bending force will break it. Wear  
631 protective glasses. Remove any under-flown cured PDMS first, and slowly remove PDMS by starting  
632 carefully, lifting the PDMS from the edges. The wafer can be re-used many times when handled  
633 properly.

634 **PAUSE POINT** The cured PDMS can be stored in a dust-free environment (petri dish) at room  
635 temperature for several months.

636 **10.** Place the PDMS on a cutting mat with the patterned side facing upward. Cut PDMS into  
637 separate microfluidic chips using a scalpel.

638 **11.** Punch with biopsy puncher (diameter 0.75 mm) into the dedicated places (inlet and outlet  
639 holes, 4 per chip. See Supplementary Data 2 for the mask for the double-sided tape to prepare the  
640 observation chamber) to make outside connections.

641 **? TROUBLESHOOTING**

642 **CRITICAL STEP** The diameter of the biopsy puncher is critical. We use a 0.75 mm-diameter biopsy  
643 puncher to make inlet holes that fits tightly a 200  $\mu$ l pipette tip (for aqueous phases, Supplementary  
644 Fig. 1) and 0.3 mm PTFE microtubing (for oil phase).

645 **12.** Cover both sides of the PDMS slab with frosted Scotch tape, and then peel off the tape from  
646 both sides to remove PDMS debris that may be formed during punching. Alternatively, dust-off the  
647 PDMS slaps with compressed air or nitrogen to remove any remaining PDMS debris.

648 **CRITICAL STEP!** Repeat step 12 if necessary. Care should be taken to remove any resulting PDMS  
649 debris or dust that can otherwise clog the microfluidic chip.

650 **13.** Place a clean glass slide and the PDMS slab in the plasma chamber with the patterned side  
651 facing upward.

652 **14.** Run the oxygen plasma program following the manufactory's recommendation. We use 30s  
653 and 35 Watts.

#### 654 ? TROUBLESHOOTING

655 **15.** Carefully remove the glass slide and PDMS slab from the plasma chamber; then bring the  
656 treated surfaces into contact. Press the PDMS slab gently onto the glass slide to ensure uniform  
657 bonding.

#### 658 ? TROUBLESHOOTING

659 **CRITICAL STEP** To avoid microfluidic channel collapse and damage, only press gently on the PDMS  
660 slab. If plasma activation is successful, the chip will attach almost by itself.

661 **CRITICAL STEP** Contact between PDMS slab and glass slide should be made quickly after plasma  
662 exposition to avoid the hydrophobic reconstitution of PDMS (< 5minutes). Be careful when placing  
663 the PDMS, once contact is established, PDMS parts cannot be moved or removed.

664 **16.** Place the microfluidic device in the oven at 90°C for 5-20 min.

665 **CRITICAL STEP** The chip needs surface treatment for the formation of droplets. Perform this step  
666 directly after plasma treatment and bonding.

667 **17.** Remove the device from the oven, and cool down at room temperature.

668 **18.** Connect a 27-gauge needle to a 0.30 mm diameter PTFE microtubing using tweezers. Fill a 1  
669 ml volume syringe with silane solution, afterwards attach a 0.22- $\mu$ m Millipore filter to the syringe.  
670 Connect the needle-microtubing to the syringe-filter and fill the whole assembly with silane solution.  
671 Prepare a second syringe filled with filtered HFE-7500 only.

672 **! CAUTION** Use tweezers to hold the tubing. Take care to not pierce your skin.

673 **! CAUTION** 1H, 1H, 2H, 2H-Perfluorododecyltrichlorosilane is corrosive and highly irritant upon  
674 inhalation. Work in a fume hood. Store the product under argon; or aliquot and freeze since the  
675 silane will react with humid air rapidly and form crystals.

676 **19.** Put the microtubing into the oil inlet and flush the microfluidic channels with silane solution  
677 for about 10-30 sec.

678 **20.** After 1-minute incubation, flush the device with compressed clean air or nitrogen.

679 **! CAUTION** Stay clear of aerosol; work under fume hood. We attach a 200  $\mu$ l pipette tip to the gas  
680 outlet to facilitate the connection.

681 **21.** Repeat steps 19 to 21 twice with pure HFE7500 oil to wash the microfluidic device.

682 **22.** Check for dust inclusion of microfluidic device using light microscopy, especially at the orifice  
683 for droplet generation. If dust is present, mark the chips and do not use them. Cover the PDMS chip  
684 with Scotch tape.

#### 685 **? TROUBLESHOOTING**

686 **PAUSE POINT** The microfluidic chip can be stored in a close box at room temperature for several  
687 months. Care should be taken to protect the devices from dust.

688

689 **Production of chamber mask in double-sided tape for the observation chamber. Timing 5 min**

690 **23.** Load the provided mask for the double-sided tape (see Supplementary Data 2 for the mask  
691 for the double-sided tape to prepare the observation chamber) into the cutting plotter.

692 **24.** Load the double-sided tape into the plotter and initiate the machine according to the user  
693 handbook.

694 **25.** Use the according plotter software (Graphtec or Silhouette Cameo) to send the design to the  
695 plotter. Use the following conditions for plotting using the Graphtec Cutting plotter:

Parameter	Setting
Offset	0
Speed	25
Acceleration	1
Cut force	21
Blade offset	2.1

696

697 And using Silhouette Cameo:

Parameter	Setting
Blade setting	3
Speed	5 cm/sec
Thickness	33

698

699 Plot the chamber design into the double-sided tape; cut with scissors into rectangles.

700 **CRITICAL STEP** The above settings will result in a plot that cuts the top protective layer and the  
701 double-sided tape, but not the bottom protective layer.

702 **PAUSE POINT** The cut tape can be stored in a close box at room temperature for several months.

703 **Production of glass slides with access holes. TIMING 5 min per slide**

704 **26.** Produce two holes (diameter around 1 mm, see Supplementary Data 3 for the mask for laser  
705 ablation) in a 76x26x1 mm microscopy slide using laser ablation. The parameters for laser ablation  
706 will depend on the type of the machine used. We use the AxysLaser with 95% energy, 20 repetitions,  
707 and cluster 10 mm to speed up the process.

708 **CRITICAL STEP** If laser ablation is not available, good alternatives are drilling, or sand-blasting. Take  
709 care to wear appropriate safety equipment when working with the glass.

710 **27.** Rinse and clean the glass slides with acetone. Repeat this process with isopropanol then  
711 clean water. Dry with compressed air or nitrogen. Clean also a glass slide without holes (for the  
712 bottom of the chamber).



713 **PAUSE POINT** The glass slides can be stored in a close box at room temperature for several months.

714

#### 715 **Microfluidic chamber assembly**

716 **28.** We use two variations of the same procedure to fabricate the droplet observation chamber.

717 When using low numbers of beads (<500 beads per droplets ; such as the sepsis application) follow

718 Option A, when using high numbers of beads (> 500 beads per droplet ; such as for the murine IgG

719 application) follow Option B. Both are based on the use of double-sided tape and glass slides. The

720 principle difference between the procedures is the equipment needed to press the chamber (binder

721 clips in Option A; thermos-press in Option B).

#### 722 **A) Sepsis application. TIMING 3-5 h**

723 **i)** Take a nanoport and place it on one of the outlet holes of the top microcopy slide (from steps 26-

724 27). Use a 23-gauge needle to align the nanoport with the access holes on the glass slide (Fig. 2c).

725 **ii)** Add a drop of a UV-curable glue at the base of the nanoport and cure with UV light.

726 **CRITICAL STEP** This step must be performed carefully to avoid the clogging of the holes. Deposit a

727 drop of viscous glue carefully which should be introduced between the slide and nanoport by

728 capillary forces (Fig. 2c). Make sure not to move the nanoport during this process.

729 **! CAUTION** Wear appropriate eye and skin protection when using UV-light to cure the glue.

730 **iii)** Repeat steps i and ii for the second hole, and then expose the glass to oxygen plasma.

731 **iv)** Cover the top slide with the patterned double-sided adhesive tape (Fig. 2c, from step 25)

732 then bring the bottom slide (from step 27) into contact to form 2D incubation chamber. Gently press

733 the glass the glass chamber to ensure uniform sealing.

734 **v)** Clamp the slides together using binder clips to seal the chamber (Fig. 2c)

735 **vi)** Incubate the clamped device for at least 2 hours at 90°C.

736 **vii)** Cool the chamber to room temperature; and remove the clamps.

#### 737 **? TROUBLESHOOTING**

738 **CRITICAL STEP** Inspect the sealing quality with an optical microscope: well-sealed device should not

739 contain Saffman-Taylor fingers (Fig. 2d).

740 **viii)** Attach a magnet onto the bottom slide of the microfluidic chamber using double-sided

741 adhesive tape (Fig. 2e). Proceed to step 28.

742 **CRITICAL STEP** The magnet is 3 mm thick, which is convenient for images acquisition using the

743 inverted microscope. Do not heat the magnet since heating may affect the magnetization.

744 **! CAUTION** This magnet is very powerful and generate a strong magnetic field (0.22T). Care should be

745 taken during handling and keep the magnet away from objects that respond to magnetic field.

746 **PAUSE POINT**

747 **B) Murine IgG application. TIMING 1.5 h**

748 i) Clean the two glass slides (top slide from steps 26-27 and bottom microscopy slide from step 27)  
749 in air plasma for 10 min. If plasma is not available, this cleaning step can be replaced with frosted  
750 scotch tape or compressed air or nitrogen.

751 ii) Remove the protective layer from the shaped double-sided tape, and put the top slide (with  
752 holes) onto the adhesive tape. Flip, remove carefully the second layer and bring the bottom slide into  
753 contact to form 2D incubation chamber. Gently press the glass chamber to ensure uniform sealing.

754 **CRITICAL STEP** Make sure to work clean and dust-free. In our experience, the tape tends to slightly  
755 adhere to the protective layers. To reduce this problem, the tape can be put at -20°C before  
756 application. Remove carefully not to rupture or form deposits of tape. Deposits of tape will result in a  
757 chamber of incorrect height and the user will observe droplet movement during measurements.

758 iii) Transfer the assembly to the thermo-press, start and heat up the thermos-press to 150°C.

759 iv) Put the assembly for 5 minutes at 150°C, and press with 7 bars to achieve a chamber with a  
760 height of  $33 \pm 2$   $\mu\text{m}$ .

761 **! CAUTION** Use appropriate safety equipment. The glass will be hot and might crack under pressure if  
762 deposits of dust, tape or other impurities are present.

763 v) Perform Step 28(A).i-ii to attach the two nanoports to the assembly.

764 vi) Attach magnets either on the side of the chamber with UV glue, or directly at the microscope  
765 using an appropriate support (see Supplementary Data 4 for the mask for the magnet holder).

766 **! CAUTION** This magnet is very powerful and generate a strong magnetic field. Care should be taken  
767 during handling and keep the magnet away from objects that respond to magnetic field. If beadlines  
768 appear to be points, the magnetic field is vertical instead of horizontal.

769 **PAUSE POINT**

770 **Surface treatment of the chamber. TIMING 10 min**

771 **29.** Repeat step 18 and then connect the tubing to the nanoport using microtight fitting adapter.

772 **30.** Flush the chamber with 0.5-1 ml silane solution, incubate for 1 to 3 minutes, completely flush  
773 with nitrogen and then fill with 1 ml HFE7500 oil. Close the assembly with two caps (Fig. 2e).

774 **! CAUTION** 1H, 1H, 2H, 2H-Perfluorododecyltrichlorosilane is corrosive and highly irritant upon  
775 inhalation. Work in a fume hood.

776 **PAUSE POINT** The chamber can be stored at room temperature for several months.

777

778 **Nanoparticle functionalization**

779 **31.** Use one of the two following approaches to functionalize the nanoparticles. One approach uses  
780 boronic acid coupling via glycosyl groups on the antibody to immobilize the antibody on the

781 nanoparticles to measure TNF- $\alpha$  secretion by single monocytes (Option A). The second approach  
782 uses the interaction between biotin and streptavidin to functionalize the beads to measure  
783 antibody secretion rate and affinity from single B cells (Option B).

784 **A) Boronic acid coupling for sepsis application. TIMING 4 h and overnight incubation**

785 **i)** Re-suspend the Carboxyl-Adembeads by pipetting and vortexing.

786 **? TROUBLESHOOTING**

787 **! CRITICAL STEP** Care should be taken to avoid foaming and bubble formation.

788 **ii)** Transfer 1 mg (33.33  $\mu$ l) of beads into a clean 1.5 ml microtube.

789 **! CAUTION** Use low binding 1.5 ml tube to perform bead functionalization.

790 **iii)** Add 100  $\mu$ l of activation buffer and vortex gently.

791 **iv)** Place the tube in a magnet holder for about 1 minute at room temperature to pellet the beads.

792 **v)** Carefully discard the supernatant using a 200  $\mu$ l pipette.

793 **! CRITICAL STEP** Do not disturb the bead pellet. A clear supernatant indicates a complete bead  
794 collection.

795 **vi)** Remove the tube from the magnet holder, and then vigorously resuspend the beads in 100  $\mu$ l  
796 activation buffer by vortexing.

797 **CRITICAL STEP** Care should be taken during washing steps. Do not allow beads to dry out. Drying  
798 reduces performances. After removing the supernatant, add buffer very quickly.

799 **vii)** Repeat steps iv – vi twice to complete the washing.

800 **viii)** Sonicate the beads for 3 minutes at room temperature at 30 W and 46 kHz. The beads are ready  
801 for EDC-sulfoNHS-based activation.

802 **CRITICAL STEP** Sonication breaks nanoparticle aggregates. The presence of aggregates reduces the  
803 efficiency of antibody coupling.

804 **! CAUTION** Wear ear protection when sonicating beads.

805 **ix)** Put aliquots of EDC and sulfoNHS (see solution setup) to room temperature for 5 to 10 minutes  
806 and prepare 10 mg/ml solution for each.

807 **x)** Mix 0.5 ml of EDC solution with 0.5 ml of sulfoNHS solution to form a solution of 5 mg/ml of  
808 activated EDC-sulfo-NHS.

809 **xi)** Place the tube containing the beads in a magnet holder for about 1 minute; and carefully discard  
810 the supernatant.

811 **xii)** Re-suspend the beads in 1 ml of activated EDC-sulfoNHS solution. Sonicate the beads for 3  
812 minutes at room temperature.

813 **xiii)** Incubate for 20 minutes on a rotating wheel at room temperature.

814 **xiv)** Place the tube in a magnet holder for 1 min to pellet the beads.

815 **xv)** Carefully discard the supernatant.

816 **xvi)** Add 100  $\mu$ l of activation buffer to the beads (see solution setup).

817 **xvii)** Remove the tube from the magnet holder and mix well by vortexing.

818 **xviii)** Repeat steps xiv – xvii twice. The beads are now activated and ready to react with boronic  
819 acid.

820 **xix)** Weigh out 50 mg of 3-Aminophenylboronic acid hemisulfate and dissolve it in 1 ml coupling  
821 buffer (later referred to as BA solution).

822 **xx)** Place the tube in a magnet holder for 1 min to pellet the beads.

823 **xxi)** Carefully discard the supernatant.

824 **xxii)** Re-suspend the beads in 1 ml BA solution, and then sonicate them for 3 minutes at room  
825 temperature.

826 **xxiii)** Incubate for 2 hours on a rotating wheel at room temperature.

827 **xxiv)** Place the tube in a magnet holder for about 3 minutes at room temperature.

828 **xxv)** Carefully discard the supernatant. Do not disturb the bead pellet.

829 **xxvi)** Add 100  $\mu$ l of PBS to beads.

830 **xxvii)** Remove the tube from the magnet holder and mix well by vortexing.

831 **xxviii)** Repeat steps xxiv - xxvii twice.

832 **xxix)** Pellet the beads by placing the microtube in a magnet holder for 1 min.

833 **xxx)** Carefully discard the supernatant. Do not disturb the bead pellet.

834 **xxxi)** Re-suspend the beads in 500  $\mu$ l of 100 mM ethanolamine to quench the reaction.

835 **! CAUTION** Ethanolamine is an irritant substance; handle it carefully under a chemical hood.

836 **xxxii)** Sonicate for 3 minutes, and then incubate 30 min at room temperature on a rotating wheel.

837 **xxxiii)** Place the tube in a magnet holder for about 1 minute at room temperature.

838 **xxxiv)** Carefully discard the supernatant. Do not disturb the bead pellet.

839 **xxxv)** Add 100  $\mu$ l of PBS to beads.

840 **xxxvi)** Remove the tube from the magnet holder and mix well by vortexing.

841 **xxxvii)** Repeat steps xxxiii - xxxvi twice.

842 **xxxviii)** Re-suspend the beads in 50  $\mu$ l PBS by vortexing, then sonicate for 3 minutes at room  
843 temperature.

844 **xxxix)** Add 50  $\mu$ g of antibody (50  $\mu$ l of 1mg/ml) to 1 mg of boronic-coated beads.

845 **! CAUTION** The anti-TNF- $\alpha$  antibody is provided in PBS buffer without sodium azide and users should  
846 work under a biological safety cabinet and aseptic conditions to avoid any contamination.

847 **CRITICAL STEP** For optimal coupling we recommend testing 10 to 50  $\mu$ g of antibody per mg of  
848 boronic-coated beads. If other antibodies are used, this optimum might be different.

849 **CRITICAL STEP** Antibody coupling will only be successful if the antibody is glycosylated.

850 **CRITICAL STEP** If other antibodies are used, these antibody solutions must be free from sodium azide,  
851 storage proteins or amine-based buffers (such as HEPES, MOPS, TRIS etc.) that could interfere with  
852 the coupling procedure. If present, the buffer needs to be exchanged using a desalting spin column  
853 or similar.

854 **xl)** Mix gently; then incubate overnight at 4 °C whilst gentle shaking.

855 **xli)** After overnight incubation, place the tube in a magnet holder for 1 min to pellet the beads.

856 **xlii)** Carefully discard the supernatant whilst not disturbing the bead pellet.

857 **xliii)** Add 100 µl of PBS to beads.

858 **xliv)** Remove the tube from the magnet holder and mix well by vortexing.

859 **xlv)** Repeat steps xli – xlv twice.

860 **xlvi)** After washing, re-suspend the beads in 200 µl storage buffer. The concentration of beads is 5  
861 mg/ml (1 mg in 0.2 ml).

862 **xlvii)** Sonicate the beads for 1 to 2 minutes at room temperature and store the Ab-coated beads at  
863 4°C.

864 **CRITICAL STEP** Keep the beads at 4 °C and do not freeze. Freezing will cause the beads to aggregate  
865 and reduces the sensitivity of the bioassay.

866 **PAUSE POINT** The antibody-coated nanoparticles are stable for at least 2 months at 4°C without  
867 affecting the performance of the bioassay. Longer storage time will need to be determined by users.

868 **xlviii)** For experiments, vortex the beads vigorously for 1 minute to re-suspend the formed pellet.

869 **xlix)** Re-suspend 10 µL of antibody-coated beads in 100 µl blocking buffer.

870 **CRITICAL STEP** Prior to using the beads in a binding assay, treat the beads with 1% dextran blocking  
871 solution (vol/vol) to reduce non-specific binding.

872 **l)** Incubate for 45 minutes at room temperature, shaking at 700 rpm.

873 **li)** Place the tube in a magnet holder for about 1 minute to pellet the beads.

874 **lii)** Carefully discard the supernatant. Do not disturb the bead pellet.

875 **liii)** Add 100 µl of PBS buffer to beads.

876 **liv)** Remove the tube from the magnet holder and mix well by vortexing.

877 **lv)** Repeat steps li – liv twice.

878 **lvi)** After the washing step, sonicate the beads for 1 min at room temperature. Use immediately for  
879 the assay.

880 **B) Biotin-streptavidin coupling for the murine IgG application. TIMING 2 h**

881 **i)** Re-suspend the Streptavidin plus-Adembeads by vortexing for 10s.

882 **? TROUBLESHOOTING**

883 **ii)** Per experiment, transfer 25  $\mu$ l of beads into a clean low-binding 1.5 ml microtube. Add 25  $\mu$ l of  
884 PBS per 25  $\mu$ l of nanoparticles.

885 **! CRITICAL STEP** Adapt accordingly if more or less nanoparticles are wanted in a droplet (see also Box  
886 1 and 2).

887 **iii)** Add 2.5  $\mu$ l of Ig immobilization reagent stock to each 50  $\mu$ l bead solution. Deposit the drop at the  
888 top of the Eppendorf, and wash down with beads. Mix by pipetting, and incubate for 20-30 min  
889 at room temperature.

890 **! CRITICAL STEP** For other biotinylated Antibodies, add 5  $\mu$ l of a 0.5 mg/ml stock to 100  $\mu$ l  
891 nanoparticles volume. This might need optimization.

892 **iv)** Pellet the beads by placing the microtube in a magnet holder for about 1 minute.

893 **v)** Carefully discard the supernatant.

894 **! CRITICAL STEP** Do not disturb the bead pellet. A clear supernatant indicates a complete bead  
895 collection.

896 **vi)** Remove the tube from the magnet holder, and then vigorously re-suspend the beads in Blocking  
897 Buffer by using the respective volume (same total volume as used in step ii). Incubate for 20-30  
898 min.

899 **CRITICAL STEP** Care should be taken during washing steps to not lose particles due to inefficient re-  
900 suspension or collection. Do not allow beads to dry out as drying reduces performance.

901 **vii)** Afterwards, repeat steps iv and v.

902 **viii)** Add Cell Buffer 1 (the same volume as used in step ii). Re-suspend the beads, and incubate for  
903 20-30 minutes to block the bead surfaces.

904 **PAUSE STEP:** The beads can be stored overnight at 4°C after this step; and used on the next day.

905 **ix)** Shortly before experiments, repeat steps iv and v.

906

### 907 **Quality control of functionalized nanoparticles**

908 **32.** Assess the binding capacity of immobilized antibody using a fluorescent-based immune-sandwich  
909 assay in microtiter plates (bulk assay; Box 4) or within droplets. For the droplet microfluidic assay  
910 for the sepsis application, follow Option A. For the droplet microfluidic assay for the murine IgG  
911 application, follow Option B.

912

913

#### 914 **A. Detection of TNF- $\alpha$ using a droplet microfluidic assay. Timing 2 h**

915 **CRITICAL:** By following this protocol and the respective dilutions, this will lead to a beadline capacity  
916 of around 3 nM within each droplet; and a number of nanoparticles of around 170 per droplet.

- 917 i. Prepare the syringes for the protein solutions by connecting a 0.56 mm diameter PTFE  
918 microtubing to 200  $\mu$ l pipette tips using PDMS slabs (6 mm diameter, with a hole in the  
919 middle of 0.75 mm diameter, see also Supplementary Fig. 1), and UV light NOA curing.  
920 Connect the tip-tubing assembly to a 27-gauge needle using tweezers, and then screw the  
921 needle to the syringe. Fill the whole system with HFE-7500.
- 922 ii. Prepare a second syringe for the reagents assay sample as described in step i.
- 923 iii. Prepare a syringe for the continuous phase by putting a 23-gauge needle on the syringe, then  
924 connect it to a 0.3 mm diameter PTFE microtubing using tweezers and fill the whole  
925 assembly with HFE-7500 oil containing 2% (wt/wt) fluorosurfactant.
- 926 **! CRITICAL STEP** Care should be taken to remove any air bubbles. If air bubbles are present,  
927 hold the syringe in a vertical position with the opening facing upwards and push the plunger  
928 until the air is completely removed.
- 929 iv. Mount the syringes on the syringe pumps and prime the assembly by applying a flow rate of  
930 1000  $\mu$ l/h for the reagent syringes to remove air bubbles from the assembly (syringes from  
931 step i and ii, reagent syringes) for about 30 seconds. The station is ready to load the samples.
- 932 v. Take antibody-coated beads from step 31(A).lvi, pipette 10  $\mu$ l of antibody-coated beads into  
933 new 1.5-ml tube and then sonicate for 3 minutes at room temperature.
- 934 **? TROUBLESHOOTING**
- 935 vi. Prepare the assay reagents for syringe 1 as follows: Add PE anti TNF- $\alpha$  antibody to a final  
936 concentration of 0.4  $\mu$ g/ml (from 20  $\mu$ g/ml stock) and antibody-coated beads at a  
937 concentration of 0.2 mg/ml (from 5mg/ml stock) in cell buffer 2. For each calibration point,  
938 prepare around 25  $\mu$ l.
- 939 **CRITICAL STEP** Centrifuge the PE anti TNF- $\alpha$  antibody at 10,000 g for 5 minutes at 4  $^{\circ}$ C to  
940 remove aggregates.
- 941 vii. For syringe 2, prepare dilutions of recombinant TNF- $\alpha$  to desired concentration in cell culture  
942 media (0-100 nM).
- 943

#### 944 **B. Detection of murine IgG using a droplet microfluidic assay. Timing 2 h**

945 **CRITICAL:** By following this protocol and the respective dilutions, this will lead to a beadline capacity  
946 of around 60 nM within each droplet, and around 1,200 nanoparticles per droplet. Each  
947 concentration counts as an experiment, so prepare a sufficient volume of beads (Step 31(B)i-ix).

- 948 **i)** Follow Step 32(A).i-iv.
- 949 **ii)** Take the functionalized nanoparticles (25  $\mu$ l of nanoparticles per experiment) from step ix  
950 (Nanoparticle functionalization, option B, Biotin-streptavidin coupling for IgG application). Collect  
951 nanoparticles, discard supernatant and re-suspend the beads in the same volume of fresh cell  
952 buffer 1. Add to the following reagents(all final concentrations): 150 nM AffiniPure F(ab')<sub>2</sub>

953 Fragment Rabbit Anti-Mouse IgG, Fcy fragment specific, 60 nM Zenon™ Alexa Fluor™ 488 Mouse  
954 IgG2b Labeling Kit; and 60 nM fluorescent antigen of interest.

955 **CRITICAL STEP** Centrifuge the fluorescent proteins at 10,000 g for 5 minutes at 4 °C to remove big  
956 aggregates before taking the solution. As for the preparation of fluorescent molecules, refer to Box 1  
957 and 2.

958 **CRITICAL STEP** Over prolonged storage time, the beads will slowly sediment. Re-suspended every  
959 hour by using a pipette.

#### 960 ? TROUBLESHOOTING

961 **iii)** For calibration, prepare a dilution series of murine calibration Ig in cell buffer 1. Start with 200  
962 nM, and divide concentration by a factor of two down to 6.25 nM. Do not forget to prepare IgG  
963 cell buffer 1 with no added IgG as a blank measure.

964 **CRITICAL STEP** Before calibrating your own antibodies, we recommend to use murine control  
965 isotypes (such as supplied by ThermoFisher) for a general calibration of the system.

966

967 **33. Generation of droplets.** Place the pipette tips of the sample syringes in a sample tube  
968 (Supplementary Fig. 1), one in the desired concentration of calibration solution and the other in  
969 the final bead solution, and aspirate 25 µl at 2000 µl/h rate of the beads and the calibration  
970 solution.

971 **34.** Connect the syringes to the corresponding inlet holes of the microfluidic device and connect the  
972 device outlet to waste with 0.30 mm diameter PTFE microtubing.

973 **35.** Set the flow rates of aqueous solutions and oil phase at 100 µl/h, then start the pumps to inject  
974 fluids into the chip. Once the droplet production is stabilized and the fluid leaves the outlet  
975 (around 8-10 µl volume used), increase the flow rate of oil to 300 µl/h to generate droplets of 50  
976 pL volume.

977 **36.** In order to collect the droplets, connect the microfluidic device outlet to the incubation chamber  
978 (from step 28(A) or 28(B) according the application) using a new piece of 0.3 mm diameter PTFE  
979 microtubing. Attach the tubing to the nanoport of the observation chamber using microtight  
980 fitting adapter. Fill the chamber with droplets (visible as a grey, homogenous and turbid layer).  
981 Once filled, remove the tubing and fluid remaining in the nanoports, and close the chamber with  
982 the caps.

#### 983 ? TROUBLESHOOTING

984 **CRITICAL STEP** The loading of the cells in a pipette tips (rather than a syringe), the encapsulation  
985 process and the chamber filling should take less than 5 min, and is typically performed at room  
986 temperature. If longer operating time is required, density-matching agents (such as OptiPrep, Percoll,  
987 Methyl Cellulose) can be added to the cell buffer. However, cells can also be cooled to 4°C to reduce



988 secretion before encapsulation in droplets, if required, though this may slow secretion rate, at least  
989 initially, after encapsulating and changing to the desired temperature for secretion measurements.  
990 To cool, a small hole is drilled or punched into the bottom of a 2 ml Eppendorf tube. The pipette tip is  
991 then introduced into the chip through the Eppendorf tube and glued in place. The volume between  
992 the pipette tip and the tube is filled with iced water during droplet loading.

993 **CRITICAL STEP** Clean the outside surfaces of the incubation chamber with isopropanol and water  
994 before filling. Apply Scotch tape to the glass chamber to remove residual dust particles.

995 **37.** Transfer the filled chamber to the microscope for imaging acquisition (Steps 38-45) and repeat  
996 steps 33-45 for all other calibration solutions.

#### 997 **? TROUBLESHOOTING**

998

#### 999 **Image acquisition. Timing 1 h**

1000 **38.** Start the epifluorescence microscope and set the heating at 37°C at least 30 minutes before  
1001 starting acquisition.

1002 **CRITICAL STEP** Care should be taken so that the experiment is performed at 37°C as the biological  
1003 responses are optimal at this temperature. Imaging at room-temperature will result in a reduced  
1004 cellular secretion rate and may also interfere with cellular secretion *per se*.

1005 **39.** Open the acquisition software and set the image acquisition program. We typically perform  
1006 quality controls of the droplets by acquiring manually a few images using a 10X objective (BF (20  
1007 ms), DAPI (300 ms - 1 sec), GFP (200 - 500 ms), CY3 (200ms - 1 sec), and CY5 (200 - 500 ms). Once  
1008 acquisition exposure times have been defined, they should not be modified for a defined assay if  
1009 a calibration curve is performed.

1010 **CRITICAL STEP** Clean the objective before imaging.

1011 **CRITICAL STEP** Exposure times will depend on the exact setup used, and may be adapted depending  
1012 on the assay and reagents used. Fix exposure time to ensure absence of saturation and optimal  
1013 fluorescence quantification.

#### 1014 **? TROUBLESHOOTING**

1015 **40.** Position the chamber on the microscope stage insert (Supplementary Fig. 2).

- 1016 - *Chamber for sepsis application:* When one magnet is attached to the chamber, place the  
1017 chamber so that the magnet is located on the left when facing the microscope; the beadline  
1018 is located in the left part of each droplet on the acquired bright-field image.
- 1019 - *Chamber for IgG application:* Position the chamber on the microscope stage insert; and place  
1020 the magnet holder above it so that the magnet is located in the front and back of the stage.  
1021 Check with bright-field: The beadline should be located in the top or bottom part of each  
1022 droplet and span over 2/3 of the droplet diameters; and should be vertical or horizontal in  
1023 orientation.

1024 **41.** Start the Perfect Focus System (PFS).

1025 **CRITICAL STEP** This step is very critical as it allows maintaining the focus at different locations of the  
1026 incubation chamber over time (corrects for potential drift of focus over time and scan).

1027 **42.** Use the bright-field channel and adjust the focus manually so that the contours of droplets and  
1028 beadlines appear as dark objects on the bright-field image (to facilitate automated detection).

1029 **CRITICAL STEP** This step is very critical since sharp focus is needed for optimal signals as well as  
1030 automated analysis.

1031 **43.** Position the objective in the middle of the incubation chamber and then set up the imaging  
1032 matrix to be acquired using the microscope software.

1033 **CRITICAL STEP** Do not acquire images close to the magnet. Before imaging and after installation of  
1034 the chamber, wait for 2-5 min for the temperature to equilibrate to reduce droplet movement due to  
1035 this difference.

1036 **44.** After the completion of the experiment, save the images as ND2 files and switch off the  
1037 microscope and the heating system.

1038 **? TROUBLESHOOTING**

1039 **45.** At this step of the protocol, quality control of the images is needed. Potential issues are  
1040 undesired movement of droplets during acquisitions, aggregation of nanobeads, irregular  
1041 distribution of beads within the droplets, presence of clusters, more than one layer of droplet  
1042 with the imaging microfluidic chamber (see Table 2 in the Troubleshooting section).

1043 **Quality control movement:** Open the images in the software, choose the bright field image and  
1044 focus on a single field of view. Activate the time-lapse function, the software will show you the  
1045 images over time. If no movement is visible ( $<1/10$  of the diameter can be tolerated), repeat this  
1046 step for two other fields of view. A small fraction of droplets ( $<2\%$ ) might rearrange their  
1047 position, these need to be removed manually or tracked.

1048 **Quality control droplets and layers:** Similarly, the presence of droplets with varying diameter  
1049 ( $>95\%$  should be similar in diameter) can be easily assessed by looking at the bright field images,  
1050 as well as the presence of multiple layers of droplets. In the former case, some data might be  
1051 useable, in the latter there is no other way than to repeat the experiment. We recommend  
1052 repeating the experiment in both cases.

1053 **Aggregation of nanobeads:** Aggregates of nanoparticles can also be seen in the bright field  
1054 image. Usually, these are potato-shaped clusters that show bright fluorescence. Therefore, also  
1055 check in the empty droplets where no secreting cell is present. These can lead to false-positive  
1056 events (see also Troubleshooting Table 2).

1057 **Irregular distribution of beads within the droplets:** This phenomenon can be checked in bright  
1058 field; and the fluorescence channels. Often, this issue is accompanied by droplets showing  
1059 different levels of fluorescence (brighter, darker droplets), and speaks for problems during  
1060 encapsulation. We recommend repeating the experiment in this case.

1061 **Presence of clusters:** The presence of cell clusters can also be checked in bright field. A relatively  
1062 easy control is to calculate the cells/droplet ratio, and compare the distribution of individual  
1063 cells/droplets with the expected distribution following Poisson. If no other issues occur, this data

1064 might still be usable, but is usually followed by an uneven distribution of dyes and antibodies as  
1065 well /see above); making its analysis difficult.  
1066  
1067  
1068

1069

1070 **Cell measurements.**

1071 **46.** The protocol can be used for a variety of different cells. The first application uses human  
1072 monocytes from healthy donors and septic shock patients (Option A), whereas the second  
1073 application uses murine IgG-secreting cells from immunized animals that were extracted from  
1074 spleen and bone marrow (Option B). Other tissues or cell types can also be analyzed. However,  
1075 cell preparation should be rapid and gentle, generating a singularized suspension of un-clumped  
1076 cells.

1077

1078 **A) Sepsis application. TIMING 5.5 h**

1079 **i)** Start the laminar flow hood for cell culture 15 minutes before starting cell extraction.

1080 **ii)** Use EasySep Direct human monocyte isolation kit from STEMCELLS technologies to isolate highly  
1081 pure CD14+ monocytes from human whole blood.

1082 **CRITICAL STEP** This protocol allows for the isolation of live cells without using density gradient  
1083 centrifugation or cell lysis buffers. For optimal recovery of monocyte isolation, use EDTA as an  
1084 anticoagulant to collect blood samples. Follow EasySep Kit instructions to isolate monocytes from 3  
1085 ml of human blood.

1086 **iii)** After the end of the EasySep protocol, pipette 7  $\mu$ l to count the cells using FastRead 102 slides.

1087 **iv)** Add 20  $\mu$ l of the fluorescently labelled anti-CD14 antibody stock to the cells to stain monocytes.

1088 **v)** Incubate for 12 minutes at room temperature in dark.

1089 **vi)** Centrifuge the cells at 2800g for 7 minutes at room temperature or 22-25  $^{\circ}$ C and carefully  
1090 remove the plasma from the cell pellet.

1091 **CRITICAL STEP** Carefully discard the supernatant. Do not disturb the cell pellet.

1092 **CRITICAL STEP** If residual red blood cells are present in the isolated cells, re-suspend the pellet in PBS  
1093 for one additional separation step. The red blood cells can be also removed by lysis using Ammonium  
1094 Chloride Solution from STEMCELL technologies (cat.no 07800).

1095 **vii)** Take antibody-coated beads from step 31(A)vi, pipette 10  $\mu$ l of antibody-coated beads into new  
1096 1.5 ml tube and then sonicate for 3 minutes at room temperature.

1097 **? TROUBLESHOOTING**

1098 **viii)** Re-suspend at  $10^6$  monocytes from step vi per 100  $\mu$ l of cell culture buffer containing 20 mM  
1099 HEPES. This is the final cell sample.

1100 **ix)** To a separate volume of cell buffer 2, add the following assay reagents (all final concentrations):  
1101 0.5  $\mu$ g/ml LPS, 0.4  $\mu$ g/ml PE anti TNF- $\alpha$ , 0.2 mg/ml antibody-coated nanoparticles, Nucview and  
1102 Mitoview probes at 2X.

1103 **? TROUBLESHOOTING**

1104

1105 **CRITICAL STEP** LPS is omitted for control experiment. Centrifuge the PE anti TNF- $\alpha$  antibody at 10,000  
1106 g for 5 minutes at 4 °C to remove aggregates.

1107 **x)** Prepare the syringes for cell sample and reagent assay samples as described in Step 32(A)i.

1108 **xi)** Prepare a syringe for the continuous phase as described in Step 32(A)iii.

1109 **! CRITICAL STEP** Care should be taken to avoid air bubble formation. If air bubbles are formed, hold  
1110 the syringe in a vertical position with the opening facing upwards and push the plunger until air  
1111 bubbles are completely removed.

1112 **xii)** Mount the syringes on the Nemesys pump and prime the assembly by applying a flow rate of  
1113 1000  $\mu$ l/h for about 50  $\mu$ l. Discard fluid. The station is ready to load the samples.

1114 **xiii)** Place the pipette tips in the sample tubes containing cell sample and assay reagents separately  
1115 (Supplementary Fig. 1) and aspirate 50  $\mu$ l at 2000  $\mu$ l/h rate.

1116 **xiv)** Connect pipette tips to the corresponding inlet holes of the microfluidic device and connect the  
1117 device outlet to waste with 0.30 mm diameter PTFE microtubing.

1118 **xv)** Set the flow rates of aqueous solutions and oil phase at 100  $\mu$ l/h then start the pumps to inject  
1119 fluids into the chip. Once droplet production is stabilized (1-2 min), increase the flow rate of oil  
1120 to 300  $\mu$ L/h to generate droplets of 50 pL volume.

1121 **? TROUBLESHOOTING**

1122 **xvi)** In order to collect the droplets, connect the microfluidic device outlet to the incubation chamber  
1123 using new PTFE microtubing. Fill the chamber with droplets (visible as a gray, homogenous and  
1124 turbid layer). Once filled, remove the tubing and fluid remaining in the nanoports, and close the  
1125 chamber with the caps.

1126 **xvii)** Immediately proceed to image acquisition as described in steps 38-45. In Step 39, use the  
1127 following image acquisition settings: BF (20 ms), DAPI (1 sec), GFP (500 ms), CY3 (1 sec), and CY5  
1128 (500 ms) images using a 10X objective. 75 fields (25x3) every 30 minutes during 3 hours (7 time  
1129 points). If a calibration curve is used for secretion, the same acquisition exposure times defined  
1130 at step 39 need to be used.

1131 **? TROUBLESHOOTING**

1132 **CRITICAL STEP** If the chamber is not clean, wipe the surfaces with ethanol, or dust off using  
1133 compressed air or scotch.

1134 **B) Murine Ig-measurements application. TIMING 2 h**

1135 **i)** Prepare spleen, bone marrow or other organs of interest according to the established protocol of  
1136 your laboratory, or follow reference<sup>38</sup>. Note that the cells should be well-suspended, and present  
1137 as individual cells to proceed and give optimal results.

1138 **CRITICAL STEP** In our experience, different protocols will result in slightly different secretion rates  
1139 that are measured. Harsh conditions and protocols, i.e. strong shear forces or chemical stress, may  
1140 result in decreased secretion rates.

1141 **ii)** Count cells in the suspension, and centrifuge the volume equivalent of 2 million of cells. Re-  
1142 suspend the cells in PBS.

1143 **iii)** Add 1  $\mu$ l/ml of CellTrace Violet (5 mM stock in DMSO); mix by pipetting and incubate the cells for  
1144 15-30 min at 37°C. Dilute the cells afterwards in cell buffer 1 to quench the reaction.

1145 **iv)** Take the beads from the assay from Step 32(B).ii

1146 **v)** Centrifuge the labelled cells at 400g for 5 min and carefully remove the supernatant from the cell  
1147 pellet. Re-suspend gently but fully at 150  $\mu$ l of Cell buffer 1. Proceed immediately to cell assay  
1148 and encapsulation.

1149 **CRITICAL STEP** The concentration of cells is optimized to result in the optimum amount of droplets  
1150 containing an individual cell. Work fast, and proceed directly to the encapsulation since the cells will  
1151 continue to secrete in bulk.

1152 **CRITICAL STEP** The cellular density is quite high in this volume. For short term (< 1-2 h), the cells can  
1153 be stored on ice. Longer storage will result in a significant decrease in Ig secretion and cellular  
1154 response.

#### 1155 **? TROUBLESHOOTING**

1156 **vi)** Prepare the syringes for cell sample, bead solution as well as continuous phase as described in  
1157 Step 32(A)i and Step 32(A)iii.

1158 **vii)** Mount the syringes on the Nemesys pumps and prime the assembly by flowing 50  $\mu$ l of solutions  
1159 with a flow rate of 1000  $\mu$ l/h. Clean the pipette tips from oil by wiping them with tissue. No air  
1160 bubbles should be visible now in the pipette tips.

1161 **viii)** Place the syringes with added pipette tips in the sample tubes (Supplementary Fig. 1), one in the  
1162 prepared cell suspension and the other in the final bead solution, and aspirate 50  $\mu$ l at 2000  $\mu$ l/h  
1163 rate of the beads and the calibration dilution.

1164 **ix)** Connect the syringes to the corresponding inlet holes of the microfluidic device.

1165 **x)** Set the flow rates of aqueous solutions and oil phase at 100  $\mu$ l/h then start the pumps to inject  
1166 fluids into the chip. Once the droplet production is stabilized, increase the flow rate of oil to 300  
1167  $\mu$ l/h to generate droplets of 50 pL volume.

#### 1168 **? TROUBLESHOOTING**

1169 **xi)** In order to collect the droplets, connect the microfluidic device outlet to the incubation chamber  
1170 using a 0.30mm diameter PTFE microtubing.

1171 **xii)** Immediately proceed to image the droplets as described in steps 38-45. In Step 39, use the  
1172 following image acquisition settings: DAPI (300 ms), GFP (200 ms), CY3 (200 ms), CY5 (200 ms)  
1173 and BF (20 ms) images using a 10X objective. 100 fields of view (10x10) every 10 minutes during  
1174 60 min (7 time points). If a calibration curve is used for secretion, the same acquisition exposure  
1175 times defined at step 39 need to be used.

1176

1177 **Automated image processing.**

1178 **47.** For image processing of data obtained for the sepsis application, follow Option A. For image  
1179 processing of data obtained for the murine IgG measurements, follow Option B.

1180

1181 **A) Sepsis application. TIMING 4 h**

1182 **i)** Extract images from ND2 files (Nikon file format) and save them in a TIFF format: 5250 images  
1183 are extracted per experiment, including both the kinetics acquired with and without LPS.

1184 **ii)** Open the input\_parameter.txt file and set the required parameters (path to the folder  
1185 containing the input images, vector of field numbers, vector of time points, various display and  
1186 saving parameters, etc).

1187 **iii)** Run the standalone Matlab application DropCell.exe  
1188 (<https://doi.org/10.6084/m9.figshare.11336663.v1>).

1189 **CRITICAL STEP** Image data without LPS and with LPS must be located in different folders and be  
1190 analyzed separately.

1191 **CRITICAL STEP** Make sure of the presence of five TIFF images per field in the input data folder,  
1192 named according to the required naming rules.

1193 **CRITICAL STEP** Make sure (by checking a few bright-field images) that the beadline is always located  
1194 in the left-hand-part of the droplets, and that its length is lower than the third of the droplets  
1195 diameter.

1196 **CRITICAL STEP** Modify the input\_parameters.txt carefully, observing format instructions.

1197 **CRITICAL STEP** Do not open Excel while running DropCell.exe.

1198 **CRITICAL STEP** Check the suitability of the analysis parameters on a few fields and time points before  
1199 running the analysis of an entire experiment.

1200 **iv)** Process the output STATdrops\_sorting\_YYYY-M-D\_H-M-S.xlsx file obtained after the  
1201 execution of DropCell.exe is completed. The Single-cell sheet focuses on the single-cell-containing  
1202 droplet. CY3 relocalization fluorescence signal (signal-to-noise ratio) per droplet and time point is  
1203 given in the columns "t\*\*\_Signal\_CY3". "trackingfail\_time", "rodfail\_time", "death\_time" and

1204 “phagocytosis\_time” columns are used, when setting appropriate filters, to select the droplets of  
1205 interest (single, live, and non-endocytic cell through the entire kinetics)

1206 **B) Murine Ig-measurements. TIMING 3-4 h**

1207 **i)** Extract images from ND2 files (Nikon file format) and save them in a TIFF format (Nikon file  
1208 format; 1 TIFF file per time point) and transfer the images to the workstation for calculation.

1209 **ii)** Open the Matlab script and run the provided script (Analyzer.m, [https://github.com/LCMD-](https://github.com/LCMD-ESPCI/dropmap-analyzer)  
1210 [ESPCI/dropmap-analyzer](https://github.com/LCMD-ESPCI/dropmap-analyzer)).

1211 **iii)** A window will pop up. Within the first line, define the channels where you want to measure  
1212 the beadline (as channel index within the file, see also readme file on the GitHub). Next, define the  
1213 bright field channel; this will be used to detect the droplets. Define the number of time points and  
1214 the average droplet radius in pixels. If you follow the protocol described herein, 25 pixels is a good a  
1215 starting point for 50 pL droplets.

1216 **CRITICAL STEP** The algorithm is sensitive to the droplet diameter you define. You might need to  
1217 increase or decrease the diameter if you change certain variables in the protocol.

1218 **iv)** The output files are a Microsoft Excel file wherein every channel is a separate sheet, sorted  
1219 by columns for beadline signal over time, average droplet signal over time and ratio of the two values  
1220 over time. In addition, Matlab file where the images of the recognized droplets are saved by index.

1221 **v)** Use the calibration curve to transfer ratios to concentration of analyte.

1222 **CRITICAL STEP** Be sure to take the right curve for the proper channel.

1223 **vi)** Please refer to Box 2 for the extraction of parameters. Sort and select droplets of interest in a  
1224 separate sheet and combine the information.

1225 **vii)** After analysis, check the selected droplets with the verify function (verify.m) to exclude false-  
1226 positive events. The verify program will show the droplets to verify their content. It will ask for a list of  
1227 indices to check.

1228 **CRITICAL STEP** Control the selected events for false-positive events (dead cells or other); and exclude  
1229 those from further analysis.

1230

1231 **Chamber cleaning after experiments. TIMING 5 min**

1232 **CRITICAL** If desired, the chambers can be used over 4-8 weeks for multiple experiments. After the  
1233 measurements, the droplets should be removed from the chamber before storage.

1234 **48.** Repeat step 18 but fill the syringe with HFE7500 oil. Connect the tubing to the nanoport using  
1235 microtight fitting adaptors.

1236 **49.** Flush the chamber with 1 ml HFE7500 oil to remove droplets.



1237 **50.** Close the nanoport chamber with caps and keep it in a dust-free environment.

1238

1239 **TROUBLESHOOTING**

1240 Troubleshooting guidance can be found in **Table 2**.

1241

1242 **Table 2. Troubleshooting Table.**

Step	Problem	Possible reason	Solution
11	Cracking in the inlets or outlets during punching.	Blunt or clogged puncher.  Insufficient mixing of PDMS and curing agent.	Use a new puncher.  Vigorously mix PDMS and curing agent to achieve a homogenous mixture of the two components. Do not cure for prolonged times (> 24 h).
14	Microfluidic device delaminates during surface treatment.	Plasma protocol was not optimal.  Not sufficiently cleaned glass slides.	Check and adapt the parameters of your plasma procedure.  Use clean glass slides: wash the glass slides with acetone, isopropanol, milli-Q water. Repeat if necessary.
15, 18-22	No droplet formation during experiments.	Collapsed microfluidic channels.  Aqueous solutions wet the microfluidics channels.  Dirt present within the microfluidic assembly.  Absence of sufficient concentration of surfactant.	Reduce force when sealing PDMS slab to glass slide.  Repeat the surface treatment of the device.  Observe microfluidic chips after fabrication for crystal formation, or the presence of dust particles.  Use HFE7500 with added 2.0% fluorosurfactant-008.

28 (A) i-vii.	Microfluidic chamber leakage.	Inefficient sealing.	Use clean glass slides and work clean. Increase the duration of incubation during step 28 (A) vi. Make sure that the nanoports are well sealed with UV glue.
36, 46 (A) xvi, 45  31 (A) i and 31 (B) i	Observed movement of droplets during acquisitions.  Aggregation of nanobeads.	Droplet coalescence occurs.  Chamber height is bigger than droplet diameter.  Presence of air within the chamber.  Microfluidic chamber is leaking.  Inherent to the beads. Long term storage of beads.	Increase the concentration of surfactant.  Fabricate a chamber with proper height (< 90% of droplet diameter). Make sure that the height of the chamber is optimal for your droplet volume.  Remove air bubbles before acquiring images.  Check steps 27 and 28 (A) i – vii.  Increase sonication time. It should be noted that extended sonication time, can heat the nanoparticles denaturing the functionalized antibodies. Ice can be added to the bath to limit nanoparticle overheating.
32 (A) i, 32 (B) i, 37, 46 A) vii	Irregular distribution of beads within the droplets, presence of clusters.	Beads aggregates during coupling.	COOH beads: increase sonication time.  Streptavidin-beads: Bead-crosslinking due to over-biotinylated immobilization reagent. After step 31 (B) iii, add 10 μM biotin before

		During storage of coupled beads.	collecting the beads. Incubate for 5-10 min before collection.  Reversible formation of clusters is normal, but should be reversible by pipetting or sonication.
BOX4 step18, 44	Failure to detect the target molecule.	Insufficient coupling efficiency.  Positive calibration samples did not result in fluorescence relocation.  In cell experiments.	Adapt concentration or incubation times. Use a fluorescent antibody to establish optimal labelling of beads. Additionally, in our experience, fluorescent analyte (TNF-A488, or Ig-A488) helps greatly to analyze problems.  Make sure that calibrate is not degraded.  Make sure of calculations of concentrations.  Make sure that no free dye is present in the fluorescent detection antibody solution. Remove free dye by centrifugation with molecular cut-off spin columns.  Use alternative method to confirm cellular secretion of the analyte (ELISA; ELISPOT; flow cytometry with brefeldin A or similar).
36, 46 (A) xvi	More than one layer of droplet is formed.	The thickness of chamber is bigger than droplet diameter.	Reduce the thickness of the chamber or increase the volume of droplets.

46 (A) xv 46 (B) i	Cell aggregates and clumps are present in the microfluidic chip during encapsulation.	Nucleic acids are released from dead cells.	Add Benzonase to cell suspension for DNA and RNA removal.
46 (A) ix 45	Cells are not fluorescent.	Cells are necrotic.  Live and dead cells staining protocol is not optimal.	Discard these cells from the analyses.  Use a probe that can detect necrotic cells.  Optimize the concentration of live/dead probes.
39-45	Rapid decrease of droplet and beadline fluorescence	Photobleaching	Optimally, reduce illumination intensity and/or exposure time.  Otherwise, reduce the total number of time points.

1243

1244

1245

1246	<b>TIMING</b>		
1247	Steps 1-22	Droplet maker fabrication	4 h
1248	Steps 23-30	Observation chamber fabrication	2-5 h
1249		Microfluidic chamber assembly	
1250		28(A) Sepsis application.	3-5 h
1251		28(B) Murine IgG application.	1.5h
1252	Steps 31(A)- 31(B)	Nanoparticle functionalization	
1253		31(A) Boronic acid coupling	4h, ON incubation
1254		31(B) Biotin-streptavidin coupling	2h
1255	Steps 32-45	Quality control of functionalized nanoparticles	
1256		BOX 4 Microtiter plate assay	3h
1257		32(A) Detection of TNF- $\alpha$ droplet assay	2h
1258		32(B) Detection of murine IgG droplet assay	2h
1259		Steps 33-45 Droplet generation and image acquisition	1h
1260	Steps 46(A) – 46(B)	Cell measurements.	
1261		46A) Sepsis Application	5.5h
1262		46B) Murine Ig-measurements application	2h
1263	Steps 47(A) – 47(B)	Automated Image processing.	
1264		47(A) Sepsis application	4h
1265		47(B) Murine Ig-measurements	3-4h
1266			

1267 **Anticipated results**

1268 The DropMap system is a flexible platform for high-throughput single-cell phenotypic analysis that is  
1269 particularly well adapted to the characterization of immune responses. The protocol can be modified  
1270 to allow the single cell quantitative analysis of a wide range of cell-surface markers and secreted  
1271 molecules expressed by a range of different cells types, simultaneously with other cellular  
1272 characteristics such as endocytosis and viability. The development described here expands its  
1273 potential from the analysis of humoral to cell-mediated and innate immune responses.

1274 The ability of DropMap to simultaneously measure secretion rates and affinities of antibodies from  
1275 thousands of single B cells makes it a powerful tool to study humoral immune responses<sup>38</sup>, for  
1276 example following vaccination<sup>71, 72</sup> or infection. Furthermore, the large data sets from these single-  
1277 cell experiments are well adapted as training sets for deep learning/artificial intelligence strategies,  
1278 and allow *in silico* modeling and simulation of the immune responses following vaccination. Such  
1279 strategies could ultimately contribute to the reduction or replacement of animal experiments.

1280 The system is also well adapted to study the role of T cells in both humoral and cell-mediated  
1281 immune responses. Given their constitutive role in immune-surveillance, aberrant T cell functions are  
1282 linked to autoimmune diseases as well as to carcinogenesis and to defective protection against  
1283 pathogen infections<sup>73, 74</sup>. In this protocol, we demonstrate our approach by integrating the  
1284 measurement of secretion of a range of murine and human cytokines produced by T cells identified  
1285 using a fluorescent anti-CD3 antibody. For example, we show here the measurement of secretion  
1286 rates of TNF- $\alpha$ , IFN- $\gamma$ , IL-2 and IL-4 from human T cells (Fig. 5, LODs of 10.4 nM, 0.6 nM, 0.5 nM and  
1287 0.2 nM for human IL-2, IL-4, TNF- $\alpha$  and IFN- $\gamma$ , respectively). Distribution of secretion rates are shown  
1288 for *ex vivo* stimulated and unstimulated peripheral blood mononuclear cells (PBMCs; stimulated with  
1289 PMA/Ionomycin).

1290 Interestingly, stimulation with PMA/ionomycin did not significantly affect the median secretion rates  
1291 for TNF- $\alpha$  (N=4 independent experiments, unstimulated  $25 \pm 13$  molecules/s; stimulated  $28 \pm 15$   
1292 molecules/s, p-value 0.77, mean  $\pm$  standard deviation of the median values for the independent  
1293 experiments, two-tailed unpaired t-test), but significantly increased the percentage of secreting T  
1294 cells by around 8-fold (from  $2.5 \pm 0.6$  % to  $17 \pm 11$  %, mean  $\pm$  standard deviation, p-value 0.05, two-  
1295 tailed unpaired t-test, Fig. 5a). In contrast, upon stimulation, there were significant increases in the  
1296 frequency and secretion rates of T cells secreting INF- $\gamma$  (N=4 independent experiments,  $1 \pm 1$  % vs.  $19$   
1297  $\pm 5$  %, p-value 0.004; and  $4.7 \pm 2.8$  molecules/s vs.  $22.5 \pm 12.8$  molecules/s, p-value 0.03, both mean  
1298  $\pm$  standard deviation of the median values for the independent experiments, two-tailed unpaired t-  
1299 test, Fig. 5b), a pro-inflammatory cytokine signature for Th1 T cells subset that is critical for fighting

1300 viral infections<sup>75-77</sup>. The average median rate of IL-2 secretion by T cells (N=3 independent  
1301 experiments,  $0 \pm 1.1$  % vs.  $24 \pm 10$  %, p-value 0.01, mean  $\pm$  standard deviation; and  $43 \pm 5$   
1302 molecules/s vs.  $73 \pm 18$  molecules/s, p-value 0.05, mean  $\pm$  standard deviation of the median values  
1303 for the independent experiments, two-tailed unpaired t-test, Fig. 5c) was equivalent with or without  
1304 stimulation, while a 10-fold increase of the frequency of IL2 secreting cells was found in the  
1305 stimulated sample. A low frequency (<2%) and low (but measurable) secretion rates (N=3  
1306 independent experiments,  $0.6 \pm 0.7$  % vs.  $1.7 \pm 0.7$  %, non-significant in a two-tailed unpaired t-test,  
1307 mean  $\pm$  standard deviation; and  $4.4 \pm 3.2$  molecules/s vs.  $4.2 \pm 2.7$  molecules/s, non-significant in a  
1308 two-tailed unpaired t-test, mean  $\pm$  standard deviation of the median values for the independent  
1309 experiments, Fig. 5d) were observed for IL-4 secreting cells in both samples. The detection of IL-4 at  
1310 low expression level in a small subset of cells nicely illustrates the advantages of DropMap, and its  
1311 use for the analysis of cytokine secretion by T cells at the single-cell level. This opens up new  
1312 opportunities to improve our fundamental understanding of immune responses, for example to  
1313 study T cell plasticity<sup>78</sup>, which may lead to the development of novel therapeutic strategies. It is also  
1314 a promising approach for clinical single-cell immuno-monitoring for patient stratification and  
1315 personalized medicine.

1316 We also extend the DropMap system to analyse the innate immune responses and to monitor the  
1317 dysfunction of monocytes from septic shock patients (Table 1). Septic shock is the most severe form  
1318 of sepsis<sup>79, 80</sup>. Sepsis is a complex clinical syndrome characterized by an early dysregulated  
1319 inflammatory response. This response, triggered by the recognition of microbial patterns by  
1320 receptors such as Toll-like receptors (TLR), is often followed by a post-infective complex immune  
1321 dysfunction combining innate and adaptive immune defects, such as monocyte dysfunction,  
1322 characterized by decreased TNF- $\alpha$  production and release<sup>81</sup>.

1323 To evaluate the potential of DropMap in this context, we first controlled its ability to maintain viable  
1324 primary human monocyte population in a confined environment over the course of an experiment  
1325 with and without pro-inflammatory lipopolysaccharide (LPS). For all experiments, only a small  
1326 fraction of cells showed apoptotic activity ( $0.49 \pm 0.09$  % for N=3 healthy donors and  $1.94 \pm 1.75$  %  
1327 for N=3 septic patients, mean  $\pm$  standard deviation for the independent experiments, Table 3),  
1328 demonstrating that the encapsulation process allows functional analysis.

1329 Deactivation of circulating monocytes is currently viewed as the soundest indicator of sepsis-induced  
1330 immunosuppression<sup>79, 80</sup> and reduced production rate of TNF- $\alpha$  by monocytes in bulk, upon *in vitro*  
1331 stimulation by LPS, is used a biomarker to monitor sepsis-induced immunosuppression in intensive  
1332 care unit patients<sup>81</sup>. However, no standardized tool is currently available in routine practice to assess



1333 the functionality of septic patients' immune system. Here, we show that the DropMap system can be  
1334 used to assess TNF- $\alpha$  secretion rate of single monocytes from septic shock patients in response to  
1335 LPS stimulation.

1336 In agreement with previous studies<sup>22</sup>, single-cell DropMap measurements revealed lower rates of  
1337 TNF- $\alpha$  secretion by monocytes upon LPS activation in septic shock patients (N=3 patients,  $1.3 \pm 0.5$   
1338 molecules/s, mean  $\pm$  standard deviation of the median values for the independent experiments)  
1339 compared to healthy donors (N=3 donors,  $2.5 \pm 1.1$  molecules/s, mean  $\pm$  standard deviation of the  
1340 median values for the independent experiments, Fig. 6a and Table 3). Without LPS, only a small  
1341 fraction (3%) of monocytes secrete TNF- $\alpha$  (N=1 donor, n=32 monocytes,  $0.9 \pm 0.4$  molecules/s, mean  
1342  $\pm$  standard deviation) demonstrating that cell activation is specifically triggered by LPS stimulation (Fig.  
1343 6b). Interestingly, the frequency of monocytes, having a TNF- $\alpha$  secretion rate below 0.5 molecules  
1344 per second (i.e. below the limit of detection of the bioassay), was higher in septic shock patients (N=3  
1345 patients,  $29 \pm 8\%$ , mean  $\pm$  standard deviation for the independent experiments), than in healthy  
1346 donors (N=3 donors,  $6 \pm 6\%$ , mean  $\pm$  standard deviation for the independent experiments). These  
1347 differences were at the limit of statistical significance ( $p=0.05$  with one-sided Mann-Whitney test)  
1348 (Fig. 6c).

1349 Furthermore, monocytes from sepsis patients have been reported to exhibit higher endocytic activity  
1350 compared to healthy donors<sup>82</sup>. The uptake of nanobeads is usually used as a readout for functional  
1351 phenotyping of cell endocytosis<sup>83-85</sup>. We thus used the DropMap platform to monitor over time the  
1352 uptake of nanobeads (endocytic activity) by monocytes. As expected, we observed differences in  
1353 nanobead uptake between cells of healthy donors (N=3 donors,  $29 \pm 3\%$ , mean  $\pm$  standard deviation  
1354 for the independent experiments) and septic shock patients (N=3 patients,  $56 \pm 15\%$ , mean  $\pm$   
1355 standard deviation for the independent experiments, Table 3). These differences were at the limit of  
1356 statistical significance ( $p=0.05$  with one-sided Mann-Whitney test). This result should be taken  
1357 cautiously given the small number of samples. Overall, these results are exemplifying the potential  
1358 application and added value of the DropMap technology in clinical studies.

1359 The DropMap system is a valuable tool for monitoring cell responses and probing heterogeneity with  
1360 single-cell resolution that can be applied in the field of immuno-monitoring, and beyond, to address  
1361 a large panel of fundamental research or clinical questions. It is robust and simple, and it can be  
1362 easily adapted to measure other cell types, in healthy and diseased states, and to measure other  
1363 secreted molecules (such as microRNAs, other cytokines, chemokines and enzymes).

1364

1365 **Table 3. Analysis of single monocytes from healthy donors and septic shock patients using**  
1366 **DropMap.**

1367 Number of LPS stimulated cells per experiment, percentage of dead cells, secretion rate  
1368 (molecules/sec), percentage of low secreting cells, and the percentage of endocytic cells of 3 healthy  
1369 donors and 3 septic shock patients. Dead monocytes were determined by measuring caspase-3  
1370 activity in droplets. Endocytic activity was assessed by counting the number of single monocytes that  
1371 bind to or internalize the magnetic beadline.

1372

	Cell number	Dead cells (%)	Secretion rate (molecules/s)	Low secreting cells (%)	Endocytic cells (%)
Healthy Donor 1	2215	0.6	3.6	1.8	31
Healthy Donor 2	3008	0.5	2.5	5.3	31
Healthy Donor 3	4495	0.4	1.4	13.3	26
Septic Patient 1	2473	1.6	0.9	34.1	61
Septic Patient 2	1122	3.8	1.9	20.0	69
Septic Patient 3	3077	0.4	1.0	31.9	39

1373

1374

1375

1376

1377 **Box 1 Assay set-up**

1378 **Choosing a pair of antibodies for the immunoassay:**

1379 When choosing a new pair of antibodies to set up another immunoassay, we use consider the  
1380 following, ranked approaches:

1381 1) Study literature and/or suppliers for antibody pairs that are tested for sandwich  
1382 immunoassays.

1383 2) A neutralizing and a non-neutralizing clone will recognize different epitopes, and binding  
1384 interference is less likely.

1385 3) The combination of polyclonal IgG for immobilization and monoclonal IgG for detection can  
1386 also show good results, although recalibration is necessary when different batches of antibody are  
1387 used.

1388 4) Use a variety of different monoclonal antibodies and test the various combinations.

1389

1390 **Labelled antigens and antibodies:**

1391 Important points to consider when preparing the reagents for the in-droplet assay:

1392 • Purify antibodies and antigens as much as possible. Pure reagents will allow for better results  
1393 and more standardized and repeatable results.

1394 • Be sure to remove any free dye or biotin before using the proteins in the assays. Any non-  
1395 bound molecules will increase the background and reduce the sensitivity of the assay. We use several  
1396 rounds centrifugation and 10K MWCO Protein Concentrators (Thermo Scientific™ Pierce™) to remove  
1397 free dyes.

1398 • When labelling the antigen with biotin or fluorescent dye, use a random method to conserve  
1399 all available epitopes on the antigen.

1400 • Do not over-label proteins. We aim for a degree of labelling (molecules/protein) of around 2.  
1401 Over-labelled antigens will not allow to set-up sensitive immunoassays.

1402 • After labelling and purification, determine the exact concentration of the protein since the  
1403 bioassay performance it highly variable with concentration.

1404 • Test the labelled proteins in an ELISA format to determine the absence of interference. For  
1405 antigens, we usually assay this by ELISA. Coat the labelled and un-labelled antigen on the ELISA plate  
1406 (separately), and add the antibody in varying concentration. Compare both binding curves.

1407

1408 **Setup concentration range:**

1409 The in-droplet assay allows for a wide range of measurements. The assay can be set up to be very  
 1410 sensitive (LOD of 500 molecules); or to span a wider concentration range. Use bulk measurements  
 1411 that help set up single-cell measurements. Look for literature values of bulk measurements that  
 1412 indicate the number of cells, time, volume and concentrations of the experiment to estimate the  
 1413 secretion rate. This crude estimation can serve as a starting point for assay set up.

1414 There are four determining factors to set up the assay: concentration of beads, immobilization  
 1415 reagent, detection reagent and the apparent dissociation constant of the pair of antibodies for  
 1416 capture and detection. For starting values, please refer to the table below.

1417

Parameter	Number of nanoparticles	Immobilization antibody	Labelled detection antibody	Apparent dissociation constant of capture and detection antibodies
Influence on capacity of the beads <sup>#</sup>	+++	+++	-	-
Influence on sensitivity <sup>#</sup>	+	+++	+++	++
Influence on measurement range <sup>#</sup>	++	++	++	+
Use of too much will result in...	Plateau in the calibration curve. Great for Yes/No answers, less suitable to quantify secretion rates	Increased waste	Decreased sensitivity; increased LOD	N.A.
Use of too little...	Absence of beadline; no reliable measurement of relocation	Plateau in the calibration curve. Great for Yes/No answers, less suitable to quantify secretion rates	Lower relocation values	N.A.
Ideally	Binding capacity matches the quantity of labelled detection reagent	Calculated as 1-2x capacity of the beads (minimized waste)	Matches capacity of beadline	As high-affinity as possible
Starting point for	170 beads	34 $\mu$ M per mg of	0.8nM	As high-affinity as

0.1-10 molecules/s (30 min assay time)	(in-droplet dilution of factor 50 from stock)	beads		possible
Starting point for 10-1000 molecules/s (0.5 hour assay time)	1,200 beads (in-droplet dilution of factor 4 from stock)	75 nM per droplet	75 nM (30 nM for antigen)	As high-affinity as possible

1418 #The magnitude of the effect is indicated: +++, strong; ++, medium; +, weak; -, no effect.

1419 - END OF BOX 1 –

1420

1421 **Box 2 Extraction of parameters**

1422 **Limit of detection:** This requires a calibration curve, a negative sample (e.g. cells not producing the  
1423 analyte, and a positive sample (e.g. cells producing the analyte).

1424 First, you will have to define a limit of detection (LOD) for the extracted secretion rate. Below this  
1425 value, you will not be able to determine whether a cell secretes the analyte. To set-up the LOD, we  
1426 recommend that you have a calibration curve, a negative sample as well as a sample (such as a cell  
1427 line) with positive events. Use the data from the calibration curve to set various thresholds, and use  
1428 them on the negative and positive samples to quantify the number of false-positives and negatives  
1429 given a certain threshold. As a starting point, we use the definition of the limit of detection (LOD) by  
1430 Armbuster and Pry<sup>86</sup> that states:

$$\text{Limit of detection (LOD)} = \overline{x_{blank}} + 1.645 * \sigma_{blank} + 1.645 * \sigma_{low}$$

1431 where  $x_{blank}$  is the mean fluorescence relocation in a negative sample,  $\sigma_{blank}$  its standard deviation and  
1432  $\sigma_{low}$  the standard deviation of a sample with low concentration. If this threshold is too low, you will  
1433 include mostly false-positives events (visible by an increased number of events in the negative  
1434 sample), whereas a too high threshold increases false-negatives (a decreased number of events in  
1435 the positive sample). If the analytical resolution is too low, set-up the assay anew with different  
1436 antibodies or concentration ranges (Box 1) and repeat the experiments.

1437 **CRITICAL:** A good labelling and high signals will decrease the limit of detection and decrease the  
1438 frequency of false-positives and negatives.

1439 **Number of cells:** Droplets with living cells are automatically detected in the analytical pathway. It is  
1440 important to have a low mean number of cells per droplet ( $\lambda < 0.2$ ) and the absence of cell clusters.

1441

1442 **Secretion rates:** This requires a calibration curve and data measured over time.

1443 Your calibration curve will consist of an increasing phase of fluorescence relocation, a plateau and an  
1444 ensuing decreasing phase, due the Hook effect (see Fig. 3b, e). Present in one-step immunoassays,  
1445 the Hook effect leads to a decrease in signal at very high analyte concentrations. In our case, at  
1446 analyte concentrations higher than beadline capacity, the non-bound analyte competes with the  
1447 bound analyte for the detection reagent; and the measured fluorescence relocation decreases.  
1448 Therefore, take care to use only the increasing phase for calculations of secretion rates in the cell  
1449 measurements. Use the fitting parameters from the calibration curve to calculate the measured in-  
1450 droplet fluorescence relocation into concentration. The secretion rate is then simply calculated by  
1451 the change of concentration over time. For each droplet followed over time, we can therefore  
1452 define:

1453 1.  $Secretion\ rate\ \left[\frac{molecules}{s}\right] = \left(\frac{1}{n-1} \left(\sum_1^{n-1} \frac{c_{i+1} - c_i}{\Delta t}\right)\right) * N_A * V$

1454 with n as the number of time points, c as the concentration present in the droplet at each time (in  
1455 pM; according to the calibration curve),  $\Delta t$  as the time difference between two measurement points,  
1456  $N_A$  as the Avogadro constant and V as the volume of the droplet (in  $\mu L$ ).

1457 **Extraction of affinity (IgG assay):** Additionally, when a fluorescent variant of the antigen of interest is  
1458 introduced into the assay, affinity of the secreted antibodies can be assayed (for more information,  
1459 see reference<sup>38</sup>). The ratio of relocated antigen fluorescence onto the beadline and free antigen  
1460 within the droplet can be used to calculate the strength of the interaction ( $K_D$ ) once the  
1461 concentration of antibody is known. This concentration is accessible using calibration curves (see  
1462 Secretion rate above). If the secreted IgG recognizes the antigen, the ratio of fluorescent antigen  
1463 bound to IgG on the beadline and mean fluorescence within the droplet can be used to calculate the  
1464 strength of the interaction ( $K_D$ ). The  $K_D$  is determined from the slope of the line defined by plotting  
1465 the relocation of fluorescent anti-IgG F(ab')<sub>2</sub> (concentration dependent) against the relocation of  
1466 fluorescent antigen to the beadline at different concentrations of IgG below the maximum capacity  
1467 of the beadline ( $\leq 50$  nM, concentration and affinity dependent).

1468 **[PRODUCTION : Please place Figure for Box 2 here].**

1469 **Measurement of murine IgG affinity.** Relocation of fluorescent antigen and fluorescent anti-IgG  
1470 detection antibody are determined by dividing the fluorescence intensity measured on the magnetic  
1471 beadline ( $I_B$ ) by the background fluorescence of the droplet ( $I_D$ ). To calculate  $K_D$ , antigen relocation  
1472 ( $I_B/I_D$  antigen) is plotted against anti-IgG detection antibody relocation ( $I_B/I_D$  anti-IgG). The slope of  
1473 this plot increases with increasing affinity, i.e. decreasing  $K_D$ . The use of several antibodies with

1474 different, but known affinities (measured, for example, using surface plasmon resonance) allows  
1475 calibration of the slope to determine  $K_D$ .

1476 Slopes of several antibodies with known affinity against the antigen are needed to calibrate the  
1477 assay. We determined the slopes for a panel of 7 purified anti-TT IgGs with affinities ranging from  
1478 300 to 0.02 nM in our initial study<sup>38</sup>, and have since reproduced this curve using a variety of different  
1479 antigens. If the antigen is multimeric, or epitopes are present more than once, an apparent  
1480 dissociation constant will be measured instead of  $K_D$ .

1481 Be aware that the slope for different isotypes (e.g. for IgG1 and IgG2) will need different calibration  
1482 curves due to their difference in fluorescence relocation<sup>38</sup>. If the slope is below 0.03; no affinity can  
1483 be detected. If the slope is above 1;  $K_D$  is at or below 0.1 nM but cannot be resolved anymore. In  
1484 order to validate the antigen and antibodies, and to make sure that the calibration curve can be used  
1485 for the system of interest, we assay 2-3 antibodies with known but different affinity; and use the  
1486 slope to calculate the  $K_D$ . The  $K_D$  should be compared with the  $K_D$  measured using an independent  
1487 method, such as Surface Plasmon Resonance.

1488 - END OF BOX 2 -

1489

### 1490 **Box 3 Distribution of cells and nanoparticles per droplet**

1491 **Cells.** In the absence of cell clusters (i.e. the cells are well individualized and suspended), the cellular  
1492 loading in this protocol follows a Poisson distribution, which is a special case of the binomial  
1493 distribution. The mean number of cells per droplet,  $\lambda$ , is determined by the number of cells in the  
1494 initial solution and the volume of an individual droplet (see the table below, 50 pL droplets). While a  
1495 higher  $\lambda$  will increase the throughput and might be advantageous to increase the number of low  
1496 frequency events, lower  $\lambda$  is preferable for single-cell measurements. Higher  $\lambda$  will increase the  
1497 frequency of droplets containing multiple cells, and data analysis needs to be adapted to cope with  
1498 these events. We usually aim for a  $\lambda$  of around 0.2-0.3, which is a compromise between maximizing  
1499 the frequency of droplets with one cell and minimizing the frequency of with multiple cells (see the  
1500 table below). We recommend validating the  $\lambda$  for each experiment by counting the number of cells in  
1501 a subset of droplets (e.g. 50 droplets) since it will also be needed to calculate the total number of  
1502 cells, and the frequency of positive events (see Box 2).

1503

Cells per ml [Mio/ml]	$\lambda$	Empty droplet	Droplets with a single cell	Droplets with multiple cells
--------------------------	-----------	---------------	--------------------------------	---------------------------------

5	0.1	90%	9.5%	0.5%
10	0.2	78%	19%	3%
20	0.4	67%	27%	6%

1504

1505 **Nanoparticles.** An advantage of the protocol described here is the co-encapsulation of single cells  
 1506 with multiple nanoparticles instead of the co-encapsulation of a single cell and a single  
 1507 microparticle<sup>35, 36</sup>. With a homogenous suspension of nanoparticles and a mean,  $\lambda$ , of hundreds to  
 1508 thousands of nanoparticles per droplet, the distribution is binomial. For the two conditions  
 1509 presented here (170 and 1,200 nanoparticles per droplet), the standard deviation is 7 and 17,  
 1510 respectively, and the coefficient of variance (CV) below 0.05. Therefore, every droplet contains  
 1511 approximately the same number of nanoparticles and the low CV assures that drop-to-drop variation  
 1512 has a minimal impact on the results. If droplets with no beads are present during analysis, these likely  
 1513 stem from errors in the flow ratios during encapsulation, due, for example, to the presence of  
 1514 clusters of beads or cells, dust in the microfluidic chips or operating errors.

1515 - END OF BOX 3 –

1516

1517 **BOX 4. Detection of protein of interest using a microtiter plate (bulk) assay. TIMING 3 h** As an  
 1518 alternative to the droplet-based quality control assays of the functionalized nanoparticles, one can  
 1519 also perform a fluorescent-based immune-sandwich assay in microtiter plates. It should be noted  
 1520 that bulk assays use more reagents and a calibration curve can also be performed directly within  
 1521 droplets to allow for the quantitative measurement of secretion rates (Box 2, Fig. 3b and e).

1522 **Procedure**

- 1523 1. Prepare a serial dilution of recombinant protein of interest (typically in the range 0-100 nM)  
 1524 in PBS containing 1% (wt/vol) BSA in a 96-well microtiter microplate. Final volumes should be  
 1525 90  $\mu$ l each.
- 1526 2. Add 10  $\mu$ l of beads to each well containing the protein of interest, and then mix well by  
 1527 pipetting.
- 1528 3. Incubate, shaking at 700 rpm, for 1 hour at room temperature.
- 1529 4. Place the microtiter plate on a magnet holder for about 1 minute at room temperature.
- 1530 5. Carefully discard the supernatant. Do not disturb the bead pellet.
- 1531 6. Add 100  $\mu$ l of PBS buffer to beads.
- 1532 7. Remove the microtiter plate from the magnet holder and mix well by vortexing.
- 1533 8. Repeat steps iv-vii once.



- 1534 9. Collect the beads, carefully discard the supernatant then add 100 µl of solution containing  
1535 0.8 µg/ml of fluorescent-labeled detection antibody to each well.
- 1536 10. Incubate, shaking at 700 rpm, for 1 hour at room temperature.
- 1537 11. Place the microtiter plate on a magnet holder for about 1 minute at room temperature.
- 1538 12. Carefully discard the supernatant. Do not disturb the bead pellet.
- 1539 13. Add 100 µl of PBS buffer to beads.
- 1540 14. Remove the microtiter plate from the magnet holder and mix well by vortexing.
- 1541 15. Repeat steps xi-xiv once.
- 1542 16. Pellet the beads using the magnet and carefully discard the supernatant. Re-suspend the  
1543 beads directly in 50 µL PBS, mix gently by pipetting.
- 1544 17. Transfer the samples to a black 96-well microtiter microplate and measure fluorescence at  
1545 the wavelength optimal for the fluorophore on the detection antibody using the microplate  
1546 reader.
- 1547 18. Plot the curve of fluorescence intensity against the concentration of added protein of  
1548 interest.

#### 1549 ? TROUBLESHOOTING

1550 - End of BOX 4-

1551  
1552  
1553

#### 1554 Acknowledgments

1555 We would like to acknowledge the support of the **REALISM study group**: HCL: André BOIBIEUX, Julien  
1556 DAVIDSON, Laure FAYOLLE-PIVOT, Julie GATEL, Charline GENIN, Arnaud GREGOIRE, Alain LEPAPE,  
1557 Anne-Claire LUKASZEWICZ, Guillaume MARCOTTE, Marie MATRAY, Delphine MAUCORT-BOULCH,  
1558 Nathalie PANEL, Thomas RIMMELE, H  l  ne VALLIN. bioM  rieux: Sophie BLEIN, Karen BRENGEL-  
1559 PESCE, Elisabeth CERRATO, Val  rie CHEYNET, Emmanuelle GALLET-GORIUS, Audrey GUICHARD,  
1560 Camille JOURDAN, Natacha KOENIG, Fran  ois MALLET, Boris MEUNIER, Marine MOMMERT, Guy  
1561 ORIOL, **Claire SCHREVEL**, Olivier TABONE, Javier YUGUEROS MARCOS. BIOASTER: J  r  mie BECKER,  
1562 Fr  d  ric BEQUET, Florian BRAJON, Bertrand CANARD, Muriel COLLUS, Nathalie GARCON, **Ir  ne**  
1563 **GORSE**, Fabien LAVOCAT, **Karen LOUIS**, Jeanne MORINIERE, Yoann MOUSCAZ, Laura NOAILLES,  
1564 Magali PERRET, Fr  d  ric REYNIER, Cindy RIFFAUD, Mary-Luz ROL, Nicolas SAPAY. SANOFI: Christophe  
1565 CARRE, Aymeric DE MONFORT, Karine FLORIN, Laurent FRAISSE, Isabelle FUGIER, Ma  na L'AZOU,  
1566 Sandrine PAYRARD, Annick PELERAUX, **Laurence QUEMENEUR**. ESPCI: **Stephanie TOETSCH**. GSK: Teri

1567 ASHTON, Peter J. GOUGH, Scott B. BERGER, David GARDINER, Aidan MACNAMARA, Aparna  
1568 RAYCHAUDHURI, Rob SMYLLIE, **Lionel TAN**, Craig TIPPLE.

1569 This research project has received funding from the French Government through the “Investissement  
1570 d’Avenir” program (grant n°ANR-10-AIRT-03) and from bioMérieux. E.K. acknowledges generous  
1571 funding from the ‘The Branco Weiss Fellowship – Society in Science’ and received funding from the  
1572 European Research Council (ERC) under the European Union’s Horizon 2020 research and innovation  
1573 programme (Grant agreement No. 80336). This work also received the support of "Institut Pierre-  
1574 Gilles de Gennes" (laboratoire d’excellence, “Investissements d’Avenir” program ANR-10-IDEX-0001-  
1575 02 PSL, ANR-10- EQPX-34 and ANR-10-LABX-31). This work was also supported by BPIFrance under  
1576 the frame "Programme d'Investissements d’Avenir" (CELLIGO Project).

1577 The authors thank the healthy donors and the septic patients who volunteered to donate peripheral  
1578 blood for these experiments. We would like to thank Marie-Noelle Unheheuer, H  l  ne Laude and  
1579 Blanca Liliana Perlaza for access to BioResources platform (ICAReB). We thank Fr  d  ric P  ne who  
1580 collected clinical samples from septic shock patients at the medical intensive care unit of Cochin  
1581 hospital (CPP17-053a / 2017-A01134-49). We thank Fabrice Porcheray for critical reading of the  
1582 manuscript.

1583 We would like to further acknowledge the help of Dr. P. Canales Herrerias and Dr. P. Bruhns for their  
1584 helpful discussion and supervision of the immunization of mice.

1585 The original data used in this publication are made available in a curated data archive at ETH Z  rich  
1586 (<https://www.research-collection.ethz.ch>) under the DOI 330317.

1587

#### 1588 **Competing interests**

1589 Some of the authors (Jean Baudry, J  r  me Bibette, Andrew Griffiths, Yacine Bounab, Christophe  
1590 V  drine) are inventors on patent applications based on certain ideas described in this manuscript and  
1591 may receive financial compensation via their employer’s rewards to inventors scheme.

1592

#### 1593 **Author Contributions**

1594 Y.B., K.E., M.R. and N.A. performed and optimized the experiments described in this protocol, S.D.  
1595 and G.C. provided the respective Matlab Scripts for data analysis, C.C and T.T. provided the statistical  
1596 tools. M.M. optimized the boronic acid nanobead functionalization protocol. CV and J.Ba. managed

1597 the optical bench set-up. J-F.L supplied the septic clinical samples. K.E, J.Bi., J.Ba and A.D.G.  
1598 developed the DropMap technology<sup>38</sup> and contributed to the early stage definition of the new  
1599 technology. Y.B. and C.V. extended DropMap technology to measure low cytokine secretion profile  
1600 and to overcome limitations of cell endocytic activity. G.M., A.P., J.T. designed and setup the clinical  
1601 study involving sepsis and matched-control patients. A.T., C.G., P.L., V.M., F.V., P.C., I.G. supervised  
1602 the work, participated to the design of technical experiments and of the clinical study and actively  
1603 contributed in writing different sections of the manuscript. Y.B., S.D. and C.V. analyzed the data for  
1604 the sepsis application, and Y.B., K.E., J.Ba., A.D.G., C.V. wrote the manuscript. All authors edited and  
1605 proof-read the paper.

1606

1607 **Code availability statement**

1608 DropMap Matlab script is available from GitHub repository, [https://github.com/LCMD-](https://github.com/LCMD-ESPCI/dropmap-analyzer)  
1609 [ESPCI/dropmap-analyzer](https://github.com/LCMD-ESPCI/dropmap-analyzer). Matlab scripts illustrating the main functions performed by the  
1610 DropCell.exe Matlab application are available from GitHub repository,  
1611 <https://github.com/bioaster/dropcell.git>. Installation file for DropCell.exe Matlab application as well  
1612 as an image data set that support/illustrate the findings of this study are available in figshare  
1613 repository, with the identifiers <https://doi.org/10.6084/m9.figshare.11336663.v1> and  
1614 [https://figshare.com/articles/dropcell\\_image\\_data\\_set/11342426](https://figshare.com/articles/dropcell_image_data_set/11342426), respectively.

1615

1616 **Data availability statement**

1617 The datasets generated during and/or analysed during the current study are not publicly available  
1618 due to confidentiality and contractual obligations towards industrial partners of the project in which  
1619 the data have been generated, but are available from the corresponding author on reasonable  
1620 request.

1621 **References**

- 1622 1. Lawson, D.A., Kessenbrock, K., Davis, R.T., Pervolarakis, N. & Werb, Z. Tumour heterogeneity  
1623 and metastasis at single-cell resolution. *Nat Cell Biol* **20**, 1349-1360 (2018).
- 1624 2. Potter, S.S. Single-cell RNA sequencing for the study of development, physiology and disease.  
1625 *Nat Rev Nephrol* **14**, 479-492 (2018).
- 1626 3. Stuart, T. & Satija, R. Integrative single-cell analysis. *Nat Rev Genet* **20**, 257-272 (2019).
- 1627 4. Svensson, V., Vento-Tormo, R. & Teichmann, S.A. Exponential scaling of single-cell RNA-seq in  
1628 the past decade. *Nat Protoc* **13**, 599-604 (2018).
- 1629 5. Zhang, X. et al. Comparative Analysis of Droplet-Based Ultra-High- Throughput Single-Cell  
1630 RNA-Seq Systems. *Molecular Cell*, 1-19 (2018).
- 1631 6. Battle, A. et al. Genomic variation. Impact of regulatory variation from RNA to protein.  
1632 *Science (New York, N.Y.)* **347**, 664-667 (2015).
- 1633 7. Peterson, V.M. et al. Multiplexed quantification of proteins and transcripts in single cells.  
1634 *Nature Biotechnology* **35**, 936-939 (2017).
- 1635 8. Shapiro, H.M. Practical Flow Cytometry. (Wiley-Liss, New York; 2003).
- 1636 9. Bendall, S.C. et al. Single-cell mass cytometry of differential immune and drug responses  
1637 across a human hematopoietic continuum. *Science (New York, NY)* **332**, 687-696 (2011).
- 1638 10. Becattini, S. et al. Functional heterogeneity of human memory CD4(+) T cell clones primed by  
1639 pathogens or vaccines. *Science (New York, N.Y.)* **347**, 400-406 (2015).
- 1640 11. Betts, M.R. et al. Sensitive and viable identification of antigen-specific CD8+ T cells by a flow  
1641 cytometric assay for degranulation. *J Immunol Methods* **281**, 65-78 (2003).
- 1642 12. Han, G., Spitzer, M.H., Bendall, S.C., Fantl, W.J. & Nolan, G.P. Metal-isotope-tagged  
1643 monoclonal antibodies for high-dimensional mass cytometry. *Nature protocols* **13**, 2121-  
1644 2148 (2018).
- 1645 13. Korin, B., Dubovik, T. & Rolls, A. Mass cytometry analysis of immune cells in the brain. *Nature*  
1646 *protocols* **13**, 377-391 (2018).
- 1647 14. Stoeckius, M. et al. Simultaneous epitope and transcriptome measurement in single cells.  
1648 *Nature methods* **14**, 865-868 (2017).
- 1649 15. Shahi, P., Kim, S.C., Haliburton, J.R., Gartner, Z.J. & Abate, A.R. Abseq: Ultrahigh-throughput  
1650 single cell protein profiling with droplet microfluidic barcoding. *Scientific reports* **7**, 44447  
1651 (2017).
- 1652 16. Czerkinsky, C.C., Nilsson, L.A., Nygren, H., Ouchterlony, O. & Tarkowski, A. A solid-phase  
1653 enzyme-linked immunospot (ELISPOT) assay for enumeration of specific antibody-secreting  
1654 cells. *Journal of immunological methods* **65**, 109-121 (1983).
- 1655 17. Kouwenhoven, M. et al. Enzyme-linked immunospot assays provide a sensitive tool for  
1656 detection of cytokine secretion by monocytes. *Clin Diagn Lab Immunol* **8**, 1248-1257 (2001).
- 1657 18. Schultes, B.C. & Whiteside, T.L. Monitoring of immune responses to CA125 with an IFN-  
1658 gamma ELISPOT assay. *J Immunol Methods* **279**, 1-15 (2003).
- 1659 19. Mogensen, T.H. Pathogen recognition and inflammatory signaling in innate immune  
1660 defenses. *Clinical microbiology reviews* **22**, 240-273, Table of Contents (2009).
- 1661 20. Garcia-Cordero, J.L., Nembrini, C., Stano, A., Hubbell, J.A. & Maerkl, S.J. A high-throughput  
1662 nanoimmunoassay chip applied to large-scale vaccine adjuvant screening. *Integrative biology*  
1663 *: quantitative biosciences from nano to macro* **5**, 650-658 (2013).
- 1664 21. Han, Q. et al. Polyfunctional responses by human T cells result from sequential release of  
1665 cytokines. *Proceedings of the National Academy of Sciences of the United States of America*  
1666 **109**, 1607-1612 (2012).
- 1667 22. Han, Q., Bradshaw, E.M., Nilsson, B., Hafler, D.A. & Love, J.C. Multidimensional analysis of the  
1668 frequencies and rates of cytokine secretion from single cells by quantitative microengraving.  
1669 *Lab on a chip* **10**, 1391-1400 (2010).
- 1670 23. Shirasaki, Y. et al. Real-time single-cell imaging of protein secretion. *Sci Rep* **4**, 4736 (2014).

- 1671 24. Son, K.J. et al. Microfluidic compartments with sensing microbeads for dynamic monitoring  
1672 of cytokine and exosome release from single cells. *The Analyst* **141**, 679-688 (2016).
- 1673 25. Varadarajan, N. et al. A high-throughput single-cell analysis of human CD8(+) T cell functions  
1674 reveals discordance for cytokine secretion and cytolysis. *The Journal of clinical investigation*  
1675 **121**, 4322-4331 (2011).
- 1676 26. Xue, Q. et al. Single-cell multiplexed cytokine profiling of CD19 CAR-T cells reveals a diverse  
1677 landscape of polyfunctional antigen-specific response. *Journal for immunotherapy of cancer*  
1678 **5**, 85 (2017).
- 1679 27. Xue, Q. et al. Analysis of single-cell cytokine secretion reveals a role for paracrine signaling in  
1680 coordinating macrophage responses to TLR4 stimulation. *Science signaling* **8**, ra59 (2015).
- 1681 28. Yamanaka, Y.J. et al. Cellular barcodes for efficiently profiling single-cell secretory responses  
1682 by microengraving. *Analytical chemistry* **84**, 10531-10536 (2012).
- 1683 29. Seah, Y.F.S., Hu, H. & Merten, C.A. Microfluidic single-cell technology in immunology and  
1684 antibody screening. *Molecular aspects of medicine* **59**, 47-61 (2018).
- 1685 30. Love, J., Ronan, J., Grotenbreg, G., Van Der Veen, A. & Ploegh, H. A microengraving method  
1686 for rapid selection of single cells producing antigen-specific antibodies. *Nat Biotechnol* **24**,  
1687 703-707 (2006).
- 1688 31. Jin, A. et al. Rapid isolation of antigen-specific antibody-secreting cells using a chip-based  
1689 immunospot array. *Nature protocols* **6**, 668-676 (2011).
- 1690 32. Köster, S. et al. Drop-based microfluidic devices for encapsulation of single cells. *Lab on a*  
1691 *chip* **8**, 1110-1115 (2008).
- 1692 33. Clausell-Tormos, J. et al. Droplet-based microfluidic platforms for the encapsulation and  
1693 screening of Mammalian cells and multicellular organisms. *Chemistry & biology* **15**, 427-  
1694 437 (2008).
- 1695 34. El Debs, B., Utharala, R., Balyasnikova, I.V., Griffiths, A.D. & Merten, C.A. Functional single-  
1696 cell hybridoma screening using droplet-based microfluidics. *Proceedings of the National*  
1697 *Academy of Sciences* **109**, 11570-11575 (2012).
- 1698 35. Mazutis, L. et al. Single-cell analysis and sorting using droplet-based microfluidics. *Nature*  
1699 *protocols* **8**, 870-891 (2013).
- 1700 36. Shembekar, N., Hu, H., Eustace, D. & Merten, C.A. Single-Cell Droplet Microfluidic Screening  
1701 for Antibodies Specifically Binding to Target Cells. *CellReports* **22**, 2206-2215 (2018).
- 1702 37. Chokkalingam, V. et al. Probing cellular heterogeneity in cytokine-secreting immune cells  
1703 using droplet-based microfluidics. *Lab Chip* **13**, 4740-4744 (2013).
- 1704 38. Eyer, K. et al. Single-cell deep phenotyping of IgG-secreting cells for high-resolution immune  
1705 monitoring. *Nat Biotechnol* **35**, 977-982 (2017).
- 1706 39. Jorgolli, M. et al. Nanoscale integration of single cell biologics discovery processes using  
1707 optofluidic manipulation and monitoring. *Biotechnol Bioeng* **116**, 2393-2411 (2019).
- 1708 40. Mocciaro, A. et al. Light-activated cell identification and sorting (LACIS) for selection of edited  
1709 clones on a nanofluidic device. *Commun Biol* **1**, 41 (2018).
- 1710 41. Winters, A. et al. Rapid single B cell antibody discovery using nanopens and structured light.  
1711 *mAbs* **11**, 1025-1035 (2019).
- 1712 42. Konry, T., Dominguez-Villar, M., Baecher-Allan, C., Hafler, D.A. & Yarmush, M.L. Droplet-  
1713 based microfluidic platforms for single T cell secretion analysis of IL-10 cytokine. *Biosens*  
1714 *Bioelectron* **26**, 2707-2710 (2011).
- 1715 43. Qiu, L. et al. A membrane-anchored aptamer sensor for probing IFN $\gamma$  secretion by  
1716 single cells. *Chem Commun (Camb)* **53**, 8066-8069 (2017).
- 1717 44. Segaliny, A.I. et al. Functional TCR T cell screening using single-cell droplet microfluidics. *Lab*  
1718 *on a chip* **18**, 3733-3749 (2018).
- 1719 45. Gérard, A., Woolfe, A. & Mottet, G., Reichen, M., Castrillon, C., Menrath, V., Ellouze, S.,  
1720 Poitou, A., Doineau, R., Briseno-Roa, L., Canales-Herrerias, P., Mary, P., Rose, G., Ortega, C.,  
1721 Delincé, M., Essono, S., Jia, B., Iannascoli, B., Richard-LeGoff, O., Kumar, R., Stewart, S.N.,  
1722 Pousse, Y., Shen, B., Gresselin, K., Saudemont, B., Sautel-Caillé, A., Godina, A., McNamara, S.,

- 1723 Eyer, K., Millot, G.A., Baudry, J., England, P., Nizak, C., Jensen, A., Griffiths, A.D., Bruhns, P.,  
1724 and Brenan. C. High-throughput single-cell activity-based screening and sequencing of  
1725 antibodies using droplet microfluidics. . *Nature Biotechnology* (In press).
- 1726 46. Duffy, D.C., McDonald, J.C., Schueller, O.J.A. & G.M., W. Rapid prototyping of microfluidic  
1727 systems in poly(dimethylsiloxane). *Analytical chemistry* **70**, 4974-4984 (1998).
- 1728 47. Anna, S.L., Bontoux, N. & Stone, H.A. Formation of dispersions using "flow focusing" in  
1729 microchannels. *Appl Phys Lett* **82**, 364-366 (2003).
- 1730 48. Akhtar, M., Driesche, S. & Vellekoop, M.J. On-chip storage of droplets in parylene-AF4 coated  
1731 PDMS channels. (2014).
- 1732 49. Di Carlo, D., Aghdam, N. & Lee, L.P. Single-cell enzyme concentrations, kinetics, and inhibition  
1733 analysis using high-density hydrodynamic cell isolation arrays. *Analytical chemistry* **78**, 4925-  
1734 4930 (2006).
- 1735 50. Jin, S.H., Jeong, H.H., Lee, B., Lee, S.S. & Lee, C.S. A programmable microfluidic static droplet  
1736 array for droplet generation, transportation, fusion, storage, and retrieval. *Lab on a chip* **15**,  
1737 3677-3686 (2015).
- 1738 51. Liu, C., Liu, J., Gao, D., Ding, M. & Lin, J.M. Fabrication of microwell arrays based on two-  
1739 dimensional ordered polystyrene microspheres for high-throughput single-cell analysis.  
1740 *Analytical chemistry* **82**, 9418-9424 (2010).
- 1741 52. Ochsner, M. et al. Micro-well arrays for 3D shape control and high resolution analysis of  
1742 single cells. *Lab on a chip* **7**, 1074-1077 (2007).
- 1743 53. Schmitz, C.H., Rowat, A.C., Koster, S. & Weitz, D.A. Dropspots: a picoliter array in a  
1744 microfluidic device. *Lab on a chip* **9**, 44-49 (2009).
- 1745 54. Duval, F., van Beek, T.A. & Zuilhof, H. Key steps towards the oriented immobilization of  
1746 antibodies using boronic acids. *The Analyst* **140**, 6467-6472 (2015).
- 1747 55. Kumar, S., Aaron, J. & Sokolov, K. Directional conjugation of antibodies to nanoparticles for  
1748 synthesis of multiplexed optical contrast agents with both delivery and targeting moieties.  
1749 *Nature protocols* **3**, 314-320 (2008).
- 1750 56. Saha, B., Evers, T.H. & Prins, M.W. How antibody surface coverage on nanoparticles  
1751 determines the activity and kinetics of antigen capturing for biosensing. *Anal Chem* **86**, 8158-  
1752 8166 (2014).
- 1753 57. Saha, B., Songe, P., Evers, T.H. & Prins, M.W.J. The influence of covalent immobilization  
1754 conditions on antibody accessibility on nanoparticles. *The Analyst* **142**, 4247-4256 (2017).
- 1755 58. Sivaram, A.J., Wardiana, A., Howard, C.B., Mahler, S.M. & Thurecht, K.J. Recent Advances in  
1756 the Generation of Antibody-Nanomaterial Conjugates. *Advanced healthcare materials* **7**  
1757 (2018).
- 1758 59. Welch, N.G., Scoble, J.A., Muir, B.W. & Pigram, P.J. Orientation and characterization of  
1759 immobilized antibodies for improved immunoassays (Review). *Biointerphases* **12**, 02d301  
1760 (2017).
- 1761 60. Dhadge, V.L., Hussain, A., Azevedo, A.M., Aires-Barros, R. & Roque, A.C. Boronic acid-  
1762 modified magnetic materials for antibody purification. *Journal of the Royal Society, Interface*  
1763 **11**, 20130875 (2014).
- 1764 61. Lin, P.C. et al. Fabrication of oriented antibody-conjugated magnetic nanoprobe and their  
1765 immunoaffinity application. *Anal Chem* **81**, 8774-8782 (2009).
- 1766 62. Wang, X., Xia, N. & Liu, L. Boronic Acid-based approach for separation and immobilization of  
1767 glycoproteins and its application in sensing. *International journal of molecular sciences* **14**,  
1768 20890-20912 (2013).
- 1769 63. Wagner, O. et al. Biocompatible fluorinated polyglycerols for droplet microfluidics as an  
1770 alternative to PEG-based copolymer surfactants. *Lab on a chip* **16**, 65-69 (2016).
- 1771 64. Williamson, J.D. & Cox, P. Use of a new buffer in the culture of animal cells. *The Journal of*  
1772 *general virology* **2**, 309-312 (1968).
- 1773 65. Lowe, K.C. Perfluorochemical respiratory gas carriers: benefits to cell culture systems. *Journal*  
1774 *of Fluorine Chemistry* **118**, 19-26 (2002).

- 1775 66. Holtze, C. et al. Biocompatible surfactants for water-in-fluorocarbon emulsions. *Lab on a chip*  
1776 **8**, 1632-1639 (2008).
- 1777 67. Mazutis, L. & Griffiths, A.D. Selective droplet coalescence using microfluidic systems. *Lab on a*  
1778 *chip* **12**, 1800-1806 (2012).
- 1779 68. Scott, R.L. The solubility of fluorocarbons. *J Am Chem Soc* **70**, 4090-4093 (1948).
- 1780 69. Simons, J.H. & Linevsky, M.J. The Solubility of Organic Solids in Fluorocarbon Derivatives.  
1781 *Journal of the American Chemical Society* **74**, 4750-4751 (1952).
- 1782 70. Qin, D., Xia, Y. & Whitesides, G.M. Soft lithography for micro- and nanoscale patterning.  
1783 *Nature protocols* **5**, 491-502 (2010).
- 1784 71. Heo, M. et al. Deep-phenotypic characterization of the immunization induced anti-bacterial  
1785 immunoglobulin-G repertoire. (submitted).
- 1786 72. Eyer, K. et al. Recall analysis as an integrative study tool of immunizations. (submitted).
- 1787 73. Raphael, I., Nalawade, S., Eagar, T.N. & Forsthuber, T.G. T cell subsets and their signature  
1788 cytokines in autoimmune and inflammatory diseases. *Cytokine* **74**, 5-17 (2015).
- 1789 74. Tanaka, A. & Sakaguchi, S. Regulatory T cells in cancer immunotherapy. *Cell Res* **27**, 109-118  
1790 (2017).
- 1791 75. Kang, S., Brown, H.M. & Hwang, S. Direct Antiviral Mechanisms of Interferon-Gamma.  
1792 *Immune Netw* **18**, e33 (2018).
- 1793 76. Mosmann, T.R., Cherwinski, H., Bond, M.W., Giedlin, M.A. & Coffman, R.L. Two types of  
1794 murine helper T cell clone. I. Definition according to profiles of lymphokine activities and  
1795 secreted proteins. *J Immunol* **136**, 2348-2357 (1986).
- 1796 77. Wheelock, E.F. Interferon-Like Virus-Inhibitor Induced in Human Leukocytes by  
1797 Phytohemagglutinin. *Science (New York, N.Y.)* **149**, 310-311 (1965).
- 1798 78. DuPage, M. & Bluestone, J.A. Harnessing the plasticity of CD4(+) T cells to treat immune-  
1799 mediated disease. *Nat Rev Immunol* **16**, 149-163 (2016).
- 1800 79. Cecconi, M., Evans, L., Levy, M. & Rhodes, A. Sepsis and septic shock. *Lancet* **392**, 75-87  
1801 (2018).
- 1802 80. Gyawali, B., Ramakrishna, K. & Dharmoon, A.S. Sepsis: The evolution in definition,  
1803 pathophysiology, and management. *SAGE Open Med* **7**, 2050312119835043 (2019).
- 1804 81. Monneret, G. et al. Novel Approach in Monocyte Intracellular TNF Measurement: Application  
1805 to Sepsis-Induced Immune Alterations. *Shock (Augusta, Ga.)* **47**, 318-322 (2017).
- 1806 82. Shalova, I.N. et al. Human monocytes undergo functional re-programming during sepsis  
1807 mediated by hypoxia-inducible factor-1alpha. *Immunity* **42**, 484-498 (2015).
- 1808 83. Kumar, P., Pai, K., Pandey, H.P. & Sundar, S. Study on pinocytosis by monocytes from visceral  
1809 leishmaniasis patients, Vol. 83. (2002).
- 1810 84. Luciani, N., Gazeau, F. & Wilhelm, C. Reactivity of the monocyte/macrophage system to  
1811 superparamagnetic anionic nanoparticles. *Journal of Materials Chemistry* **19**, 6373-6380  
1812 (2009).
- 1813 85. Robert, D. et al. Cell sorting by endocytotic capacity in a microfluidic magnetophoresis  
1814 device. *Lab on a chip* **11**, 1902-1910 (2011).
- 1815 86. Armbruster, D.A. & Pry, T. Limit of blank, limit of detection and limit of quantitation. *Clin*  
1816 *Biochem Rev* **29 Suppl 1**, S49-52 (2008).

1817

## 1818 **FIGURE LEGENDS**

1819 **Figure 1. Single cell secretion assay in microfluidic droplets.** (a) Co-encapsulation of cells and assay  
1820 reagents into picoliter droplets. Red arrows show individual cells in droplets. Scale bars 50  $\mu\text{m}$  (b, c)  
1821 Principle of the single-cell secretion assay in droplets. The bioassay comprises magnetic nanoparticles

1822 (300 nm diameter) functionalized with capture antibodies, and fluorescently-labeled detection  
1823 antibodies. In the absence of secreted analyte (**b**), no binding occurs on the magnetic beadline and  
1824 the fluorescent signal remains homogenous within the droplet. In the presence of secreted analyte  
1825 (**c**), antibody-coated beads capture the secreted analyte and the fluorescent signal becomes  
1826 relocalized to the beadline, due to the fluorescently-labelled detection antibody binding the captured  
1827 analyte. Black arrows (B->) below the droplet indicate the direction of the magnetic field that induces  
1828 beadline formation in the droplets. Both scale bars 25  $\mu\text{m}$ . (**d**) A brightfield image of beadlines and  
1829 monocytes in a compact array of 50 pL droplets. Scale bar 50  $\mu\text{m}$ . (**e**) Complete chip design used to  
1830 co-encapsulate cells and reagents. Scale bar 750  $\mu\text{m}$ .

1831

1832 **Figure 2. Fabrication of the microfluidic glass chamber using double-sided adhesive tape.** (**a**)  
1833 Dimensions of the lower and upper glass slides enclosing the chamber. The upper slide contains two  
1834 1 mm wide holes. Droplets are injected through one hole (the other one acting as a vent). (**b**)  
1835 Dimensions of the adhesive tape and pattern of the chamber. (**c**) Key steps for droplet chamber  
1836 fabrication (step numbers refer to the steps described in the Procedure section of the manuscript).  
1837 (**d**) Brightfield images of the glass/tape composite: Saffman-Taylor fingers are formed at room  
1838 temperature (RT); they are not formed after a 90°C incubation (28(A).vi) . (**e-f**) Device composition:  
1839 two glass slides (at bottom and top) sealed with the double-sided adhesive tape, two inlet/outlet  
1840 nanoports (in the top glass slide, sealed with two caps), and a magnet glued to the bottom glass slide  
1841 (alternative chamber fabrication 1).

1842

1843 **Figure 3. Characterization of functionalized nanoparticles in droplets.** (**a**) Schematic representation  
1844 of nanoparticle coating for TNF- $\alpha$  detection. The bioassay comprises paramagnetic nanobeads  
1845 functionalized with anti-TNF- $\alpha$  antibodies using boronic acid coupling to glycosyl groups. (**b**)  
1846 Detection of human recombinant TNF- $\alpha$  in 50 pL droplets. The relocation of the fluorescently-labeled  
1847 detection antibodies in the presence of different concentrations of TNF- $\alpha$ . The signal was determined  
1848 by dividing the fluorescence intensity measured on the magnetic beadline ( $I_B$ ) by the background  
1849 fluorescence of the droplet ( $I_D$ ). Top left, brightfield image. Bottom left, fluorescent image. Right,  
1850 signal ( $I_B/I_D$ ) as a function of TNF- $\alpha$  concentration. (**c**) Time courses of TNF- $\alpha$  secretion by individual  
1851 monocytes. Each curve represents the kinetic signal of a single cell. Top left, brightfield image.  
1852 Bottom left, fluorescent image. Right, signal ( $I_B/I_D$ ) as a function of time, each curve represents the  
1853 signal of a single cell. Black lines indicate the relocation within droplets with non-secreting cells. (**d**)  
1854 Schematic representation of nanoparticle coating for IgG detection. The bioassay comprises  
1855 paramagnetic nanobeads functionalized with anti-mouse kappa light chain  $V_{\text{H}}\text{H}$  that capture IgG onto



1856 the bead surface. (e) Detection of murine recombinant IgG1 (circles) and IgG2 (squares) in 50 pL  
1857 droplets. Top left, brightfield image. Bottom left, fluorescent image. Right, signal ( $I_B/I_D$ ) as a function  
1858 of IgG concentration (IgG1 detection reagent, red lines; IgG2 detection reagent, green lines). (f) Time  
1859 course analyses of IgG secretion of individual B cells. Top left, brightfield image. Bottom left,  
1860 fluorescent image. Right, signal ( $I_B/I_D$ ) as a function of time, each curve represents the mean signal of  
1861 a single cell (IgG1, red lines; IgG2, green lines). Black lines indicate the relocation within droplets with  
1862 non-secreting cells. All scale bars are 25  $\mu\text{m}$ .

1863

1864 **Figure 4. Analysis pipeline.** (a) Acquisition of images of the monolayer of droplets, illustrated for a  
1865 single field of view in 5 imaging channels. Measurements were repeated at regular time intervals. (b)  
1866 Detection of droplet contours in the field, and of the intra-droplet beadline (bright-field image) (c).  
1867 Tracking of droplets allows continued analysis in spite of potential small droplet movements  
1868 (supplementary Fig. 3 and supplementary method 1). (d) Images illustrating multiplexed and dynamic  
1869 analyses of single monocytes. The droplet sub-image is shown in the five different imaging channels.  
1870 Bright-field is used to detect droplets and magnetic beadlines, a Cy3 cube (orange fluorescence) is  
1871 used to detect the secreted TNF- $\alpha$  on the beadline, a Cy5 cube (far red fluorescence) is used to  
1872 detect living cells, a GFP cube (far-red fluorescence) is used to detect dead cells, and a DAPI cube  
1873 (blue violet conjugate fluorescence) is used to detect cells expressing the cell surface marker CD14.  
1874 The CD14 positive monocytes remained alive over 180 min and TNF- $\alpha$  relocalization on the beadline  
1875 is detected 60 min after stimulation in droplets at 37°C. At 180 min, the cell shows an apoptotic  
1876 activity indicating the death of the cell. Live and dead monocytes were determined by staining with  
1877 MitoView and NucView to measuring mitochondrial membrane potential and caspase-3 activity,  
1878 respectively. Scale bar 50  $\mu\text{m}$ .

1879

1880 **Figure 5. Analysis of cytokine secretion from human single T cells.** (a) Distribution of the frequencies  
1881 of TNF- $\alpha$  (17 $\pm$ , (b) IFN- $\gamma$ , (c) IL-2 and (d) IL-4 secreting T cells (identified using a fluorescent FITC-  
1882 conjugated anti-CD3 antibody) in PMA/ionomycin stimulated human PBMCs (orange) and non-  
1883 stimulated PBMCs (black). Panels a and b depict 4,515 cells for stimulated, and 7'525 cells for non-  
1884 stimulated PBMCs. Panels c and d depict 8,640 and 8,606 individually assayed cells for stimulated  
1885 and non-stimulated cells respectively. The data represents a single experiment. No or only little  
1886 secretion was found in the population of CD3 negative cells. Gray bars represent the part of the  
1887 distribution that could not be analyzed due to the LOD of the assays (see also Box 1 and 2).

1888

1889 **Figure 6. Analysis of TNF- $\alpha$  secretion from human single monocytes of healthy donor and septic  
1890 shock patient.** (a) Distribution of the frequencies of TNF- $\alpha$  secreting monocytes upon LPS stimulation

1891 of a healthy donor (black line, 3008 cells) and septic shock patient (orange line, 2473 cells). **(b)**  
1892 Distribution of the frequencies of TNF- $\alpha$  secreting monocytes upon LPS stimulation (black line, 3008  
1893 cells) and non-stimulated cells (dashed line, 1099 cells) of a healthy donor. Low secreting cells exhibit  
1894 TNF- $\alpha$  secretion rate below 0.5 molecules per second. The data represents a single experiment. Gray  
1895 bars (a and b) represent the part of the distribution that could not be analyzed due to the LOD (TNF-  
1896  $\alpha$  secretion rate below 0.5 molecules per second) of the assay (see also Box 1 and 2). **(c)** Percentage  
1897 of low secreting monocytes of septic patients (N=3 patients, black squares,  $29 \pm 8\%$ , mean  $\pm$  standard  
1898 deviation for the independent experiments) and healthy donors (N=3 donors, black circles,  $6 \pm 6\%$ ,  
1899 mean  $\pm$  standard deviation for the independent experiments). Error bars show standard deviation-  
1900

1901

## 1902 **List of supplementary information**

1903 **Supplementary Figure 1.** Explanatory figure for steps 33-35 to assemble the tip connectors and the  
1904 syringes for the aqueous phases.

1905 **Supplementary Figure 2.** Explanatory figure for step 40 to position the chamber on the microscope  
1906 stage insert.

1907 **Supplementary Figure 3.** Explanatory figure describing the pipeline analysis of droplet detection and  
1908 tracking.

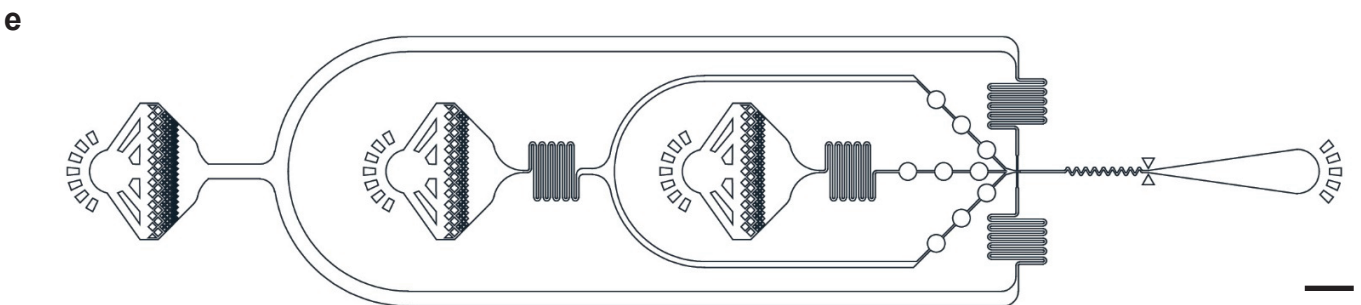
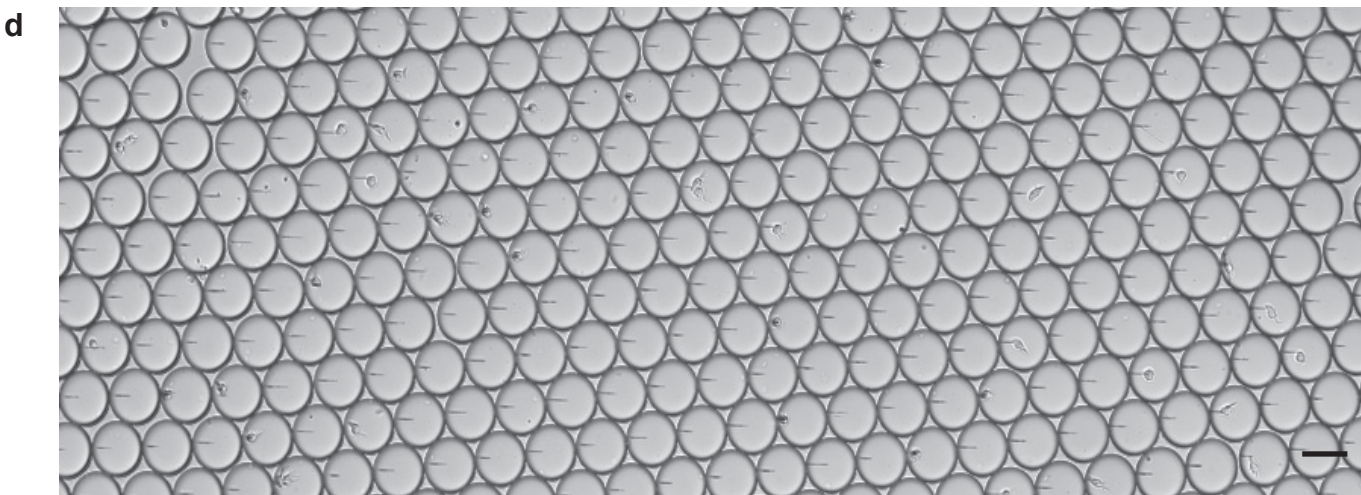
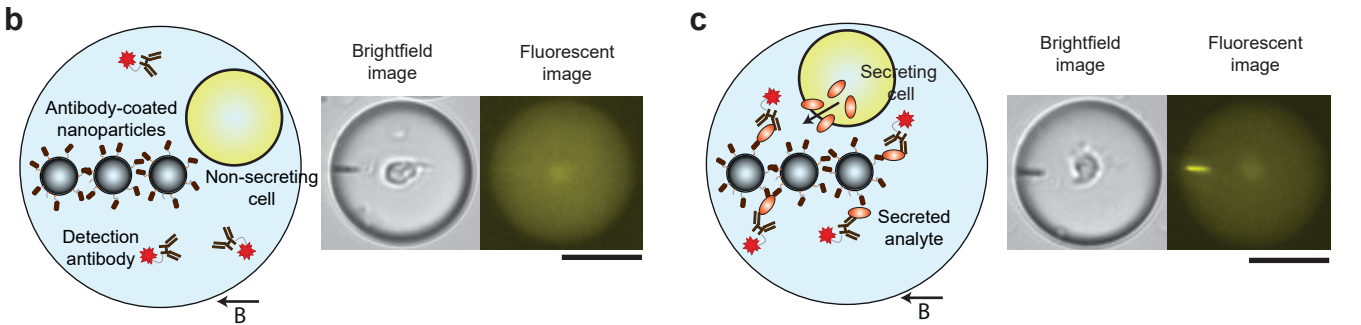
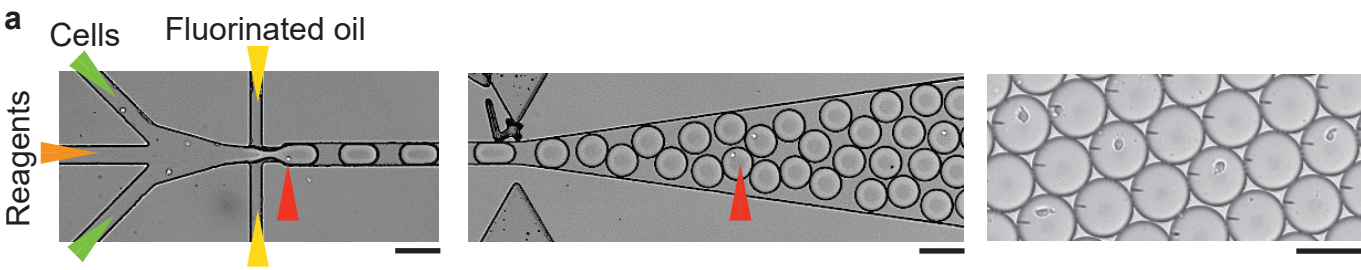
1909 **Supplementary Method 1.** Pipeline analysis of droplet detection and tracking.

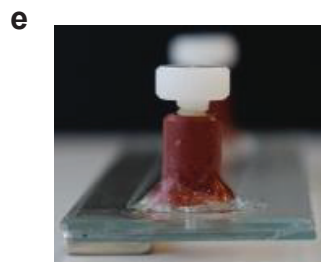
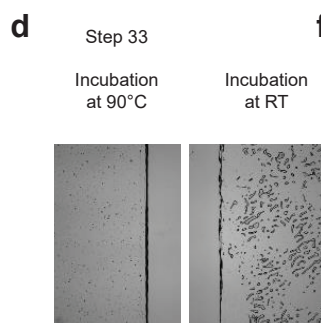
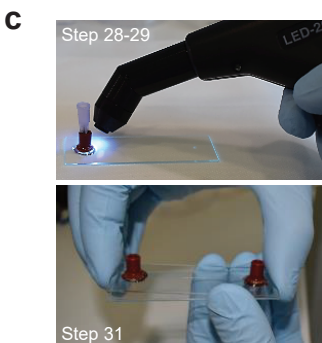
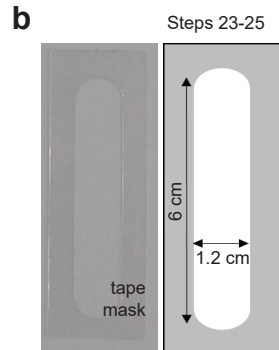
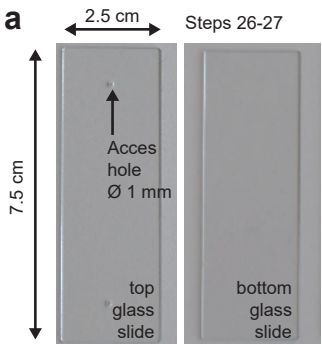
1910 **Supplementary Data 1.** Complete chip design (CAD file).

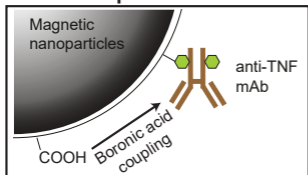
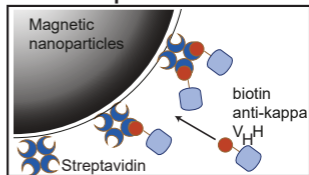
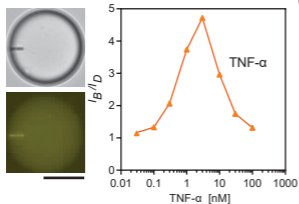
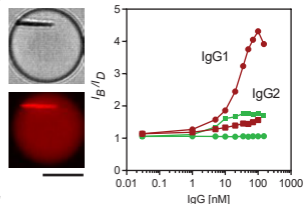
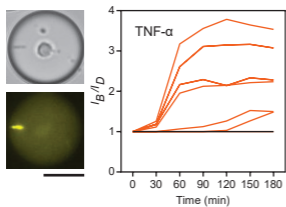
1911 **Supplementary Data 2.** Mask for the double-sided tape to prepare the observation chamber.

1912 **Supplementary Data 3.** Mask for laser ablation.

1913 **Supplementary Data 4.** Mask for the magnet holder.





**a** Steps 47-102**d** Steps 103-111**b****e****c****f**